Department of Neuroscience and Biomedical Engineering

Improving the reliability of transcranial magnetic stimulation targeting

Aino Nieminen

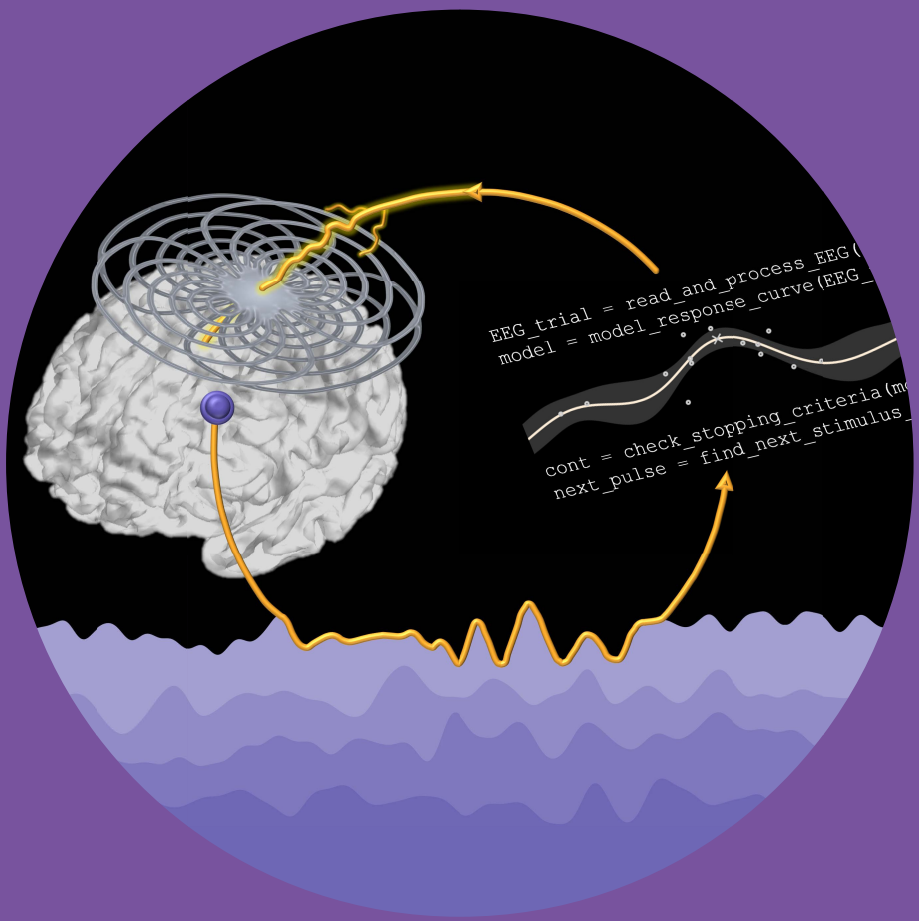

Aalto University

DOCTORAL THESES

Aalto University publication series
DOCTORAL THESES 77/2022

Improving the reliability of transcranial magnetic stimulation targeting

Aino Nieminen

A doctoral thesis completed for the degree of Doctor of Science (Technology) to be defended, with the permission of the Aalto University School of Science, at a public examination held at the lecture hall F239a (Otakaari 3) on 29 June 2022 at 12 noon.

Aalto University
School of Science
Department of Neuroscience and Biomedical Engineering

Supervising professor
Prof. Risto Ilmoniemi, Aalto University, Finland

Thesis advisors
Dr. Jaakko Nieminen, Aalto University, Finland
Dr. Selja Vaalto, Aalto University and Helsinki University Hospital, Finland

Preliminary examiners
Prof. Srinivasa Chakravarthy, Indian Institute of Technology Madras, India
Prof. Axel Thielscher, Technical University of Denmark and Copenhagen University Hospital Hvidovre, Denmark

Opponent
Prof. Fabio Babiloni, Sapienza University of Rome, Italy

Aalto University publication series
DOCTORAL THESES 77/2022

© 2022 Aino Nieminen

ISBN 978-952-64-0820-0 (printed)
ISBN 978-952-64-0821-7 (pdf)
ISSN 1799-4934 (printed)
ISSN 1799-4942 (pdf)
http://urn.fi/URN:ISBN:978-952-64-0821-7

Unigrafia Oy
Helsinki 2022

Finland

NORDIC SWAN ECOLABEL
Printed matter
4041-0619

Aalto University

Abstract

Aalto University, P.O. Box 11000, FI-00076 Aalto www.aalto.fi

Author
Aino Nieminen

Name of the doctoral thesis
Improving the reliability of transcranial magnetic stimulation targeting

Publisher School of Science

Unit Department of Neuroscience and Biomedical Engineering

Series Aalto University publication series DOCTORAL THESES 77/2022

Field of research Biomedical Engineering

Manuscript submitted 8 March 2022 **Date of the defence** 29 June 2022

Permission for public defence granted (date) 11 May 2022 **Language** English

☐ **Monograph** ☒ **Article thesis** ☐ **Essay thesis**

Abstract

Neurons in the human brain can be locally activated with transcranial magnetic stimulation (TMS). TMS is applied to study brain dynamics, to map cortical functions, and to treat neurological and psychiatric disorders. In TMS, an electric field is induced in the brain. The location of the electric field maximum is targeted with a neuronavigation system that shows the coil placement and the peak electric field on a brain image. To find a suitable stimulation location and orientation, the TMS operator gives pulses with varying stimulus parameters and observes the responses, such as muscle twitches upon stimulating the motor cortex. This mapping procedure is, however, operator-dependent and slow. In addition, TMS navigation systems are not error-free. Inaccuracies and variation in TMS methods can cause varying results that may be difficult to interpret and compare.

This Thesis aimed at increasing the reliability of TMS targeting by developing automated targeting methods. Publication 1 presents an algorithm to automatically identify the best stimulation location and orientation in the motor cortex, i.e., the stimulus parameters that maximize the motor responses measured with electromyography. In Publication 2, a similar closed-loop approach was applied to search for the optimal stimulus orientation but now with electroencephalography as a feedback signal.

Automated procedures require a way for non-manual adjustment of TMS parameters. In Publications 1 and 2, the stimulus location or orientation was electronically controlled with a 2-coil multi-locus TMS, which concurrently drives two overlapping coils. By adding more coils into the system, one can extend the electronically adjustable parameter space. This was realized in Publication 3 with a 5-coil device, which enabled a demonstration of an automated mapping of the hand motor area with predefined stimulus locations and orientations.

Publication 4 aimed at analyzing errors related to TMS navigation systems. The simulations showed that the magnitudes of the errors in navigation depend on the methods employed. The operator can ensure reliable TMS navigation by performing related preparations carefully and by selecting the most accurate methods for navigation.

The automated procedures developed in this Thesis allow operating TMS in a fast and user-independent way, increasing the reliability of TMS. Moreover, the closed-loop algorithms pave the way for adaptive TMS treatments, i.e., the real-time adjustment of the TMS delivery with observed effects so that the clinical outcome is maximized. This, together with accurate navigation, is expected to increase the efficacy of TMS therapy, bringing help to patients suffering from brain dysfunctions.

Keywords transcranial magnetic stimulation, electromyography, electroencephalography, neuronavigation, closed-loop, Bayesian optimization

ISBN (printed) 978-952-64-0820-0 **ISBN (pdf)** 978-952-64-0821-7

ISSN (printed) 1799-4934 **ISSN (pdf)** 1799-4942

Location of publisher Helsinki **Location of printing** Helsinki **Year** 2022

Pages 120 **urn** http://urn.fi/URN:ISBN:978-952-64-0821-7

Tekijä
Aino Nieminen

Väitöskirjan nimi
Transkraniaalisen magneettistimulaation kohdistamisluotettavuuden parantaminen

Julkaisija Perustieteiden korkeakoulu

Yksikkö Neurotieteen ja lääketieteellisen tekniikan laitos

Sarja Aalto University publication series DOCTORAL THESES 77/2022

Tutkimusala Lääketieteellinen tekniikka

Käsikirjoituksen pvm 08.03.2022 **Väitöspäivä** 29.06.2022

Väittelyluvan myöntämispäivä 11.05.2022 **Kieli** Englanti

☐ **Monografia** ☒ **Artikkeliväitöskirja** ☐ **Esseeväitöskirja**

Tiivistelmä

Aivojen hermosoluja voidaan aktivoida paikallisesti transkraniaalisen magneettistimulaation (TMS) avulla. TMS:ää käytetään hermoverkkojen dynamiikan tutkimukseen, aivotoimintojen kartoitukseen sekä neurologisten sairauksien hoitoon. TMS:ssä aiheutetaan sähkökenttäpulssi aivoihin. Sähkökentän huippukohta kohdistetaan neuronavigaatiosysteemin avulla, joka näyttää stimulaatiokelan asettelun sekä sähkökentän aivokuvan päällä. Löytääkseen sopivan stimulaatiokohdan ja -suunnan, TMS:n käyttäjä aktivoi aivoja eri parametrein ja seuraa niistä aiheutuvia vasteita, kuten lihasnykäisyjä liikeaivokuorta stimuloitaessa. Tämä kartoitusprosessi on kuitenkin käyttäjäriippuvaista ja hidasta. TMS:n navigointisysteemitkään eivät ole virheettömiä. Epätarkkuudet ja eroavaisuudet TMS-menetelmissä voivat johtaa vaihteleviin tuloksiin, joita on hankala tulkita ja vertailla.

Tämän väitöskirjan tavoitteena oli lisätä TMS:n kohdistustarkkuutta kehittämällä automatisoituja kartoitusmenetelmiä. Osatyössä 1 esitellään algoritmi optimaalisen stimulaatiopaikan ja -suunnan määrittämiseen. Algoritmilla etsittiin automaattisesti sellaiset stimulaatioparametrit, joiden avulla saatiin suurimmat lihassähkökäyrällä mitatut vasteet. Osatyössä 2 käytettiin samanlaista algoritmia optimaalisen stimulaatiosuunnan etsintään, mutta lihasvasteiden sijaan takaisinkytkentäsignaalina oli aivosähkökäyrä.

Automatisoidut TMS-prosessit vaativat ei-manuaalisen tavan TMS-parametrien säätöön. Osatöissä 1 ja 2 stimulaatiosuuntaa ja -paikkaa säädettiin sähköisesti kaksikelaisen monipaikka-TMS:n avulla, jossa käytetään samanaikaisesti kahta päällekkäin olevaa stimulaatiokelaa. Päällekkäin olevien kelojen määrää lisäämällä voidaan kasvattaa sähköisesti ohjattavaa parametrialuetta. Tällainen toteutettiin osatyössä 3 viiden kelan systeemikokonaisuutena, joka mahdollisti käden edustusalueen automaattisen kartoituksen etukäteen valituilla stimulaatiopaikoilla ja -suunnilla.

Osatyön 4 tavoitteena oli analysoida TMS-navigointiin liittyviä virheitä. Työn simulaatiot osoittivat, että navigaatiovirheiden suuruus riippuu käytetyistä menetelmistä. TMS-käyttäjä voi kuitenkin varmistaa luotettavan TMS-navigoinnin suorittamalla siihen liittyvät valmistelut huolella sekä valitsemalla navigointiin tarkimmat saatavilla olevat menetelmät.

Tässä väitöskirjassa kehitetyt automatisointimenetelmät mahdollistavat TMS:n käytön nopealla ja käyttäjäriippumattomalla tavalla lisäten TMS:n luotettavuutta. Takaisinkytkentäalgoritmit luovat pohjaa TMS-hoitojen reaaliaikaiseen mukauttamiseen eli siihen, että TMS:ää säädetään hoidon aikana mitattujen vasteiden perusteella. Yhdessä tarkan navigointijärjestelmän kanssa, automatisoidun reaaliaikaisen säätämisen odotetaan lisäävän TMS-hoitojen tehokkuutta ja tuovan apua aivosairauksista kärsiville potilaille.

Avainsanat transkraniaalinen magneettistimulaatio, lihassähkökäyrä, aivosähkökäyrä, neuronavigaatio, automaattinen säätö, Bayesilainen optimointi

ISBN (painettu) 978-952-64-0820-0 **ISBN (pdf)** 978-952-64-0821-7

ISSN (painettu) 1799-4934 **ISSN (pdf)** 1799-4942

Julkaisupaikka Helsinki **Painopaikka** Helsinki **Vuosi** 2022

Sivumäärä 120 **urn** http://urn.fi/URN:ISBN:978-952-64-0821-7

Preface

In December 2013, I sent an email inquiring possible Bachelor's Thesis topics to an Academy Professor running several fascinating projects on developing technologies for studying and treating the human brain. After only a couple of hours, I sat in the office of that professor and left with an offer to work in his lab. Through the following years, interesting projects followed one another, and I found myself staying in the lab longer than initially planned. To the professor in question, Aalto Distinguished Prof. Risto Ilmoniemi: thank you for your trust and the inspiring atmosphere in which to make science. To my Thesis advisor Dr. Jaakko Nieminen: enormous thanks for the pleasant collaboration, happy times in the lab, and all the help in challenges throughout this journey. Dr. Selja Vaalto, I appreciate your support as an advisor and in providing insights in the clinical importance of this work.

It has also been an honor to have other bright co-workers in the projects included in my Thesis. It was a privilege to have Prof. Jukka Sarvas, who is no longer with us, as my math mentor. Jukka's help was invaluable, and I admired his enthusiasm and ability to always learn new things. I highly value agreeable teamwork and conversations with Dr. Johanna Metsomaa. Dr. Matti Stenroos, I appreciate your work in teaching and collaborating in various aspects of electromagnetism. Thank you for the relevant questions and unhurried chats in the office. Dr. Pantelis Lioumis, I give thanks to the endless idea generator who put up with me and my measurement company for so many hours in the lab. Dr. Victor Souza, I value the fruitful discussions and the long but joyful measurements we have had. The other co-authors Heikki Sinisalo, Mikko Malmi, Dr. Mikhail Yuryev, Diego Milardovich, Dr. Juuso Korhonen, Dr. Lari Koponen, Dr. Pavel Novikov, Dr. Maria Nazarova, and Dr. Vadim Nikulin, I am pleased to have had all of you in the team. I am also grateful to the other current and former members of the TMS group, the international projects, and the department for the stimulating environment to make research in. In addition, I express my gratitude to the personnel of BioMag Laboratory and AMI Centre for making it possible to carry out the experiments in their facilities.

I want to thank the pre-examiners Prof. Srinivasa Chakravarthy and Prof. Axel Thielscher for taking their time to review my Thesis and for providing constructive suggestions to make this Thesis clearer. Moreover, I am grateful to Prof. Fabio Babiloni for accepting the request to act as the opponent at the public defense of my Thesis.

I acknowledge the funding sources enabling to work full time towards this Thesis. I appreciate the personal funding from the Aalto Brain Centre, Finnish Cultural

Foundation, and Instrumentarium Science Foundation. In addition, I value funding from the Academy of Finland (decisions No. 294625, 306845, and 327326) and European Research Council (ERC Synergy, European Union's Horizon 2020 research and innovation programme, ConnectToBrain, grant agreement No. 810377).

I am grateful to my family and friends for their support and encouragement through the years. I appreciate the work of my former teachers especially in math and physics, as they have ignited my enthusiasm to study and work in the engineering field. My bio-fellow and friend Dr. Elsi Verrinder, I am indebted to you for your peer support in all aspects of studies, work, and life during these years at Aalto. Dear Jaakko, when starting this work, I would never have imagined that you would become the closest person to me. Thank you for your love. I am so fortunate in having you by my side in all the future adventures.

Espoo, May 20, 2022,

Aino Nieminen

Contents

List of abbreviations

ADM	Abductor digiti minimi
APB	Abductor pollicis brevis
DBS	Deep brain stimulation
DES	Direct electrical stimulation
DLPFC	Dorsolateral prefrontal cortex
EEG	Electroencephalography
E-field	Electric field
EMG	Electromyography
FDA	U.S. Food and Drug Administration
FDI	First dorsal interosseus
ISO	International Organization for Standardization
M1	Primary motor cortex
MEP	Motor-evoked potential
MRI	Magnetic resonance imaging
MT	Motor threshold
mTMS	Multi-locus transcranial magnetic stimulation
nTMS	Navigated transcranial magnetic stimulation
PET	Positron emission tomography
rTMS	Repetitive transcranial magnetic stimulation
tACS	Transcranial alternating current stimulation
TEP	TMS-evoked potential
TES	Transcranial electrical stimulation
TMS	Transcranial magnetic stimulation

List of publications

This doctoral dissertation of Aino Nieminen (née Tervo) consists of a summary and of the following publications, which are referred to in the text by their numerals.

1. **Tervo, Aino E.**; Metsomaa, Johanna; Nieminen, Jaakko O.; Sarvas, Jukka; Ilmoniemi, Risto J., 2020. *Automated search of stimulation targets with closed-loop transcranial magnetic stimulation.* NeuroImage, 220, 117082. https://doi.org/10.1016/j.neuroimage.2020.117082

2. **Tervo, Aino E.***; Nieminen, Jaakko O.*; Lioumis, Pantelis; Metsomaa, Johanna; Souza, Victor H.; Sinisalo, Heikki; Stenroos, Matti; Sarvas, Jukka; Ilmoniemi, Risto J., 2022. *Closed-loop optimization of transcranial magnetic stimulation with electroencephalography feedback.* Brain Stimulation, 15, 523–531. https://doi.org/10.1016/j.brs.2022.01.016

3. Nieminen, Jaakko O.*; Sinisalo, Heikki*; Souza, Victor H.; Malmi, Mikko; Yuryev, Mikhail; **Tervo, Aino E.**; Stenroos, Matti; Milardovich, Diego; Korhonen, Juuso T.; Koponen, Lari M.; Ilmoniemi, Risto J., 2022. *Multi-locus transcranial magnetic stimulation system for electronically targeted brain stimulation.* Brain Stimulation, 15, 116–124. https://doi.org/10.1016/j.brs.2021.11.014

4. **Nieminen, Aino E.**; Nieminen, Jaakko O.; Stenroos, Matti; Novikov, Pavel; Nazarova, Maria; Vaalto, Selja; Nikulin, Vadim; Ilmoniemi, Risto J., 2022. *Accuracy and precision of navigated transcranial magnetic stimulation.* Under review.

* These authors contributed equally to the work.

Author's contribution

Publication 1: *Automated search of stimulation targets with closed-loop transcranial magnetic stimulation*
All authors conceptualized the study and participated in planning the methodology. **AET**, JM, and JON carried out the experiments. **AET** and JM analyzed the data. **AET**, JM, JON, and JS contributed to the algorithm and data analysis software. **AET** prepared the figures. **AET** and JM wrote the initial draft of the manuscript. All authors reviewed and edited the manuscript.

Publication 2: *Closed-loop optimization of transcranial magnetic stimulation with electroencephalography feedback*
AET, JON, PL, JM, and RJI conceptualized the work. **AET**, JON, PL, JM, and JS designed the methodology. **AET**, JON, PL, and VHS performed the measurements. **AET**, JON, and JS implemented the algorithm. **AET** analyzed the data with software input from JM, VHS, and MS. MS made the head models. **AET** made the visuals with help from MS. AET wrote the initial version of the manuscript. All authors reviewed and edited the manuscript.

Publication 3: *Multi-locus transcranial magnetic stimulation system for electronically targeted brain stimulation*
JON, HS, VHS, LMK, and RJI conceptualized the work. JON, HS, VHS, **AET**, MS, and LMK designed and implemented the methodology. JON, HS, VHS, MM, MY, DM, JK, and LMK designed the mTMS system. JON, HS, VHS, and MM manufactured and characterized (measurements and analysis) the device. JON, HS, and **AET** planned and executed the motor mapping experiment. JON analyzed the motor mapping data. JON, HS, VHS, and MS made the illustrations. JON, HS, and VHS wrote the first version of the manuscript with input from MS. All authors reviewed and edited the manuscript.

Publication 4: *Accuracy and precision of navigated transcranial magnetic stimulation*
All authors conceptualized the study. **AEN**, JON, MS, and PN designed the methodology. **AEN** made the coregistration error simulations with software input from PN. **AEN** and MS made the E-field simulations with software input from JON. **AEN**, JON, and MS prepared the figures. **AEN** and JON wrote the draft of the manuscript with input from MS, MN, and SV. All authors reviewed and edited the manuscript.

1. Introduction

The brain, our most complex organ, enables a multitude of vital body functions such as senses and muscle movements. Neural tissue consists of brain cells of which the most important ones are neurons, as they are responsible for the encephalic electrochemical information processing. The human brain contains over 80 billion neurons meaning that they are about 10 times more numerous than the earth's population. Additionally, each neuron is connected to even thousands of other nerve cells via synapses forming a complex network. This network is active all the time through electrical impulses (such as action potentials) and synaptic activity. The brain is constantly stimulated, for example, by senses, i.e., the cerebral cortex gets information from the sensory systems, which modifies the electrical activity of the brain.

The cortical activity can be also artificially altered by various, mainly electromagnetic, brain stimulation methods. Neural tissue can be directly and effectively stimulated with direct electrical stimulation (DES) and deep brain stimulation (DBS). They, however, require opening or drilling the skull. One can also feed electric current to the brain with electrodes on the scalp; this is called transcranial (meaning that the stimulation penetrates the skull) electrical stimulation (TES). The current strength one can tolerate in TES is not, however, able to trigger action potentials in most cases. Instead, transcranial magnetic stimulation (TMS) can painlessly and noninvasively generate action potentials.

TMS is increasingly employed and has applications in brain research, diagnostics, and therapy. TMS hardware and methods have been developed and diversified since its introduction, and supporting systems have been integrated with TMS, for example, to target and navigate the stimuli based on anatomical brain images. Although TMS systems can be highly advanced, there is still room for improvements. For example, navigation methods are not error-free and a typical TMS protocol involves manual and operator-dependent procedures. In addition, TMS requires adjusting many parameters, and it is often unknown what is the best way to deliver TMS when studying cortical functions or treating brain disorders. These aspects can lead to varying TMS outcomes and reduced reliability of TMS hindering wider adoption of the method.

This Thesis helps to recognize and understand different sources of errors and variation in TMS methods and provides detailed analyses on the targeting reliability. In addition, this Thesis presents new methods for automating TMS procedures. Automation reduces especially user-dependent errors and variability and has potential for making TMS even more reliable and effective.

This Thesis is organized so that Chapter 2 presents the aims of this work, Chapter 3 introduces the basics of TMS, Chapter 4 provides insights on the reliability of TMS, Chapter 5 describes the elements required for automating TMS, and Chapter 6 summarizes the publications included in this Thesis. The Thesis ends with a discussion of the results presented (Chapter 7) and conclusions (Chapter 8).

2. Aims of the Thesis

The aim of this Thesis was to increase understanding about the reliability of TMS targeting and improve it. This aim is reflected in the goals of the publications included in this Thesis as follows:

1) The aim of Publications 1–3 was to automate TMS procedures to make them more reliable and faster. More specifically, the goal of Publications 1 and 2 was to automate the stimulation guiding based on recorded motor and brain responses, respectively. The aim of Publication 3 was to demonstrate fast and easy TMS mapping of the motor cortex.

2) The goal of Publication 4 was to analyze quantitatively the errors related to TMS navigation methods to help TMS users in understanding how different error sources and methodological choices can affect the reliability of their TMS results.

3. Transcranial magnetic stimulation

This chapter introduces the basics of TMS. I first describe how TMS activates the brain and how pulses are targeted to desired places on the cortex. Then, I will explain how the electrophysiological responses to TMS can be measured with electromyography (EMG) and electroencephalography (EEG). In addition, I will give examples of the applications of TMS.

3.1 Basic principles

In TMS, a stimulation coil formed of loops of copper wire is placed against the head, and a brief intense electric current pulse is fed through the coil windings by discharging a capacitor in the TMS circuit (for a review, see, e.g., Ilmoniemi et al. (1999)). The current flow generates a magnetic field $\vec{B}$ in the surroundings, with the strength of the field decreasing with distance from the coil. As the current circulating in the coil changes as a function of time, so does the magnetic field. This means that also an electric field (E-field), which depends on the location $\vec{r}$ and time t, is produced, as stated by Faraday's law

$$\nabla \times \vec{E}_{\mathrm{p}}(\vec{r}, t) = -\frac{\partial \vec{B}(\vec{r}, t)}{\partial t}. \tag{3.1}$$

$\vec{B}$ can be expressed with magnetic vector potential $\vec{A}$ as $\vec{B} = \nabla \times \vec{A}$. We can, thus, write

$$\vec{E}_{\mathrm{p}}(\vec{r}, t) = -\frac{\partial \vec{A}(\vec{r}, t)}{\partial t}. \tag{3.2}$$

In conducting medium, such as the head, the primary E-field ($\vec{E}_{\mathrm{p}}$) produces a current

$$\vec{J}_{\mathrm{p}}(\vec{r}, t) = \sigma(\vec{r})\vec{E}_{\mathrm{p}}(\vec{r}, t) \tag{3.3}$$

that depends on the conductivity $\sigma(\vec{r})$.

Conductivities in the head vary from tissue to tissue, leading to charge accumulation on conductivity borders and to charge density $\rho(\vec{r}, t)$. This effect develops a secondary E-field ($\vec{E}_{\mathrm{s}}$) that is formulated in Gauss's law

$$\nabla \cdot \vec{E}_{\mathrm{s}}(\vec{r},t) = \frac{\rho(\vec{r},t)}{\varepsilon_0}, \tag{3.4}$$

where ε_0 is the vacuum permittivity. Under the quasistatic approximation, the electric field can be expressed with the help of scalar potential V as follows:

$$\vec{E}_{\mathrm{s}}(\vec{r},t) = -\nabla V(\vec{r},t). \tag{3.5}$$

After computing $\vec{E}_{\mathrm{p}}$, one can solve V from the continuity equation

$$\nabla \cdot \vec{J}(\vec{r},t) = -\nabla \cdot \sigma(\vec{r})\nabla V(\vec{r},t) + \nabla \cdot \sigma(\vec{r})\vec{E}_{\mathrm{p}}(\vec{r},t) = 0 \tag{3.6}$$

and further $\vec{E}_{\mathrm{s}}$. In a simplistic approach, the head can be modeled as a sphere, and the secondary TMS E-field has an analytical formula (Heller and van Hulsteyn, 1992). More realistic head models require numerical methods and discretization of the head geometry into small volume elements, as with the finite element method (Thielscher et al., 2011; Windhoff et al., 2013), or surface elements, as with the boundary element method (Nummenmaa et al., 2013; Salinas et al., 2009).

The total induced E-field ($\vec{E} = \vec{E}_{\mathrm{p}} + \vec{E}_{\mathrm{s}}$) accumulates charge also on neuronal cell membranes. This changes the membrane potential; if it is increased (depolarized) enough, an action potential is triggered. TMS can activate neuron populations and elicit, for example, a muscle twitch when stimulating suitable site on the primary motor cortex (Barker et al., 1985). However, exact activation mechanisms and locations in the brain are still under investigation. Generally, it is thought that the activation occurs at the cortical area where the E-field has its maximum (Ilmoniemi et al., 1999), although neuronal cells can get activated also on areas with weaker magnitudes in E-field profile. It has been suggested that at least on the motor cortex, pyramidal cells are directly activated at the axon hillock (Baker et al., 1995) or axonal terminations (Aberra et al., 2020) in the gray matter or bending site of the neuron in the white matter (Maccabee et al., 1993) when the pulse is strong enough. With lower intensities, possible muscle twitches likely result from the activation of interneurons that have synaptic connections to pyramidal cells (Di Lazzaro et al., 2004; Laakso et al., 2014).

3.2 Navigated TMS

TMS stimuli can be targeted to a relevant cortical place with desired orientation with the help of image-guided neuronavigation systems (Comeau, 2014; Hannula and Ilmoniemi, 2017; Herwig et al., 2001; Ruohonen and Karhu, 2010). In navigated TMS (nTMS), the coil placement and the estimated E-field maximum are visualized on top of an anatomical brain image (typically magnetic resonance image, MRI). This can be done when the relative placement of the head and the coil is known. In addition to guiding in the targeting of certain anatomical structures, a navigation system is of help when the same stimulation needs to be repeated and it also records information about the administered pulses.

Figure 1 shows an example of a neuronavigation system. An nTMS system includes a tracking unit, often an infrared camera or an electromagnetic tracker, capable of following certain markers in 3D space. Trackable markers are attached to the head of the subject and to the TMS coil, enabling the monitoring of head and coil locations and movements in real time. The coordinates of the head and the MRI of the subject are aligned in a procedure called registration. During registration, certain points from the physical head are recorded with a separate digitizer tool and matched to the corresponding points in the MRI. A similar process is done for the coil and its 3D model. TMS navigation systems also include a program that coregisters TMS and MRI, i.e., combines the recorded spatial information to show the coil placement in the MRI coordinates.

As the E-field maximum is thought to associate with the cortical site of stimulation, navigation systems typically show an estimate of it. The simplest estimation approach is called line navigation, in which the location of the E-field maximum is approximated as a cortical site that intersects with a line passing through the center of the coil bottom in a perpendicular direction (Herwig et al., 2001). Some systems compute the E-field with a spherical model, giving more accurate information about the location and orientation of the E-field maximum (Hannula and Ilmoniemi, 2017; Ruohonen and Karhu, 2010). E-field navigation systems also provide the magnitude of the cortical E-field maximum.

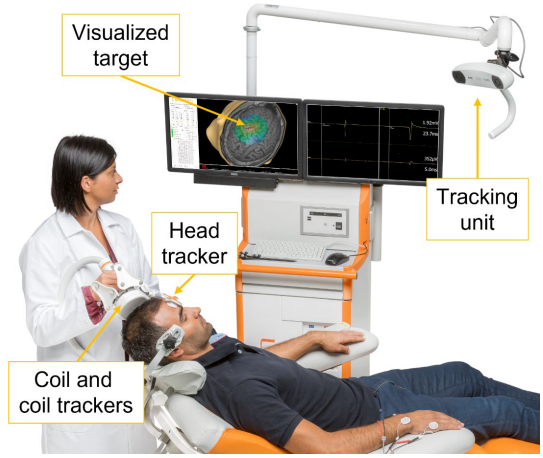

Figure 1. A navigated TMS system. The main parts of the system are a coil with coil trackers, head tracker, tracking unit with infrared cameras, and software visualizing the TMS-induced E-field on the top of an MRI. Photo courtesy of Nexstim Plc.

3.3 TMS and electromyography

TMS-induced motor responses called motor-evoked potentials (MEPs) can be measured with EMG (Barker et al., 1985). In EMG, potential differences (voltages) due to electrical muscle activity are measured on the skin surface with a pair of

electrodes: one electrode is attached on top of a muscle, and another one, for example, on top of a tendon or bone for reference (see Fig. 2B). A ground electrode helps to reduce common-mode noise.

TMS-evoked MEPs (see Fig. 2C) in hand muscles begin about 20 ms after the TMS pulse and the peak-to-peak amplitude of MEPs can be several millivolts. MEP amplitudes depend on the TMS intensity, but the amplitudes can vary a lot from trial to trial even with fixed stimulus intensity. A common MEP measure is the motor threshold (MT), which is defined as the stimulus intensity that evokes an MEP above a certain amplitude (typically 50 μV) with 50% probability. When EMG measurements are combined with stimulus sites recorded by a TMS navigation system, one can create a map of the MEP amplitude as a function of the stimulus location.

Figure 2. Measuring motor responses with electromyography. **A**: Stimulus location and orientation on the hand-knob area of the left motor cortex. The orange dot indicates the location of the E-field maximum, and the red arrow shows the direction of the strongest E-field. **B**: EMG electrodes to measure responses from the *first dorsal interosseus* muscle of the right hand. Photo by Aleksi Poutanen. **C**: An example of an MEP response. A TMS pulse was given at 0 ms.

3.4 TMS and electroencephalography

TMS induces local and global changes in the brain activity. These changes can be detected with EEG, which measures electric potentials on the scalp (see Fig. 3). Neural signals in EEG are thought to reflect mainly postsynaptic potentials in pyramidal neurons on the cortex (Ilmoniemi and Sarvas, 2019; Kirschstein and Köhling, 2009). A postsynaptic potential is generated when an action potential arrives at a synapse and neurotransmitters are released, causing current flow into or out from the neuron to which the synapse is attached. The effect of a TMS pulse on an EEG signal appears as a series of deflections time-locked to the TMS pulse. This response lasting a few hundreds of milliseconds is called a TMS-evoked potential (TEP). TEPs can be used to study cortical excitability and how the induced activity propagates in the brain (Farzan et al., 2016; Ilmoniemi et al., 1997).

The first TMS–EEG measurements employed only a few electrodes (Amassian et al., 1992; Cracco et al., 1989). Later, with TMS-compatible EEG, higher-density measurements covering a large part of the cortex became possible (Ilmoniemi et al., 1997). Due to the strong magnetic pulses applied, successful TMS–EEG measurements require TMS-compatible electrodes and amplifiers (Ilmoniemi and Kičić, 2010; Vernet and Thut, 2014; Virtanen et al., 1999). Despite the advances in EEG

devices, TMS–EEG signals can contain various large-amplitude artifacts, such as electromagnetic, electrode movement, and muscle artifacts covering the neural signals of interest (Ilmoniemi et al., 2015; Mutanen et al., 2013; Vernet and Thut, 2014). Artifacts need to be taken into account and minimized when possible during the measurements (Casarotto et al., 2022) and in data processing (Mutanen et al., 2020, 2018; Rogasch et al., 2017).

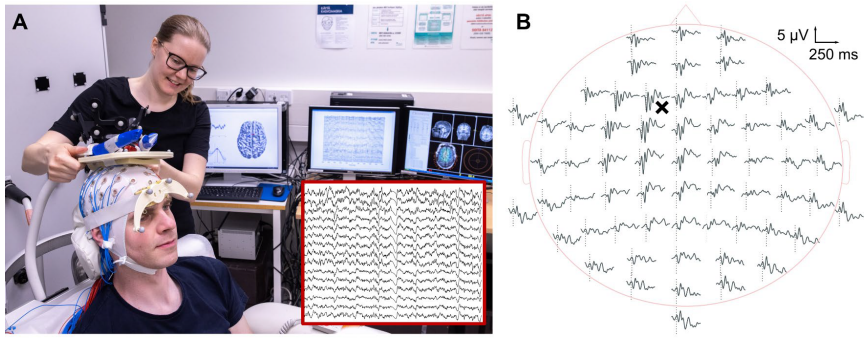

Figure 3. Measuring brain responses with electroencephalography. **A**: TMS–EEG measurement setup with raw EEG signals on the bottom right. Photo by Mikko Raskinen (Aalto University). **B**: Examples of TMS-evoked potentials after stimulating left pre-supplementary motor area. The stimulation site is marked with a black cross.

3.5 Applications of TMS

TMS has various applications in scientific and clinical settings (Rossini et al., 2015). In brain research, TMS provides a unique way to study cerebral dynamics and mechanisms, especially when combined with EMG or EEG. When complemented by a navigation system, TMS enables convenient mapping of cortical functions, such as motor movements and speech (Krieg et al., 2017). By giving two TMS pulses with a millisecond-scale time interval, one can study the inhibitory and facilitatory mechanisms of the brain networks, i.e., the influence of interneurons in modulating the functioning of pyramidal neurons (Di Lazzaro, 2013; Ziemann et al., 1996). In addition, cognitive processes can be investigated with TMS, as suitably targeted TMS can disturb or enhance subject's performance during cognitive tasks (Pascual-Leone et al., 2000; Walsh and Cowey, 2000).

In clinical settings, TMS is applied in diagnostics especially in diseases related to the motor system (Groppa et al., 2012). Planning of neurosurgery can benefit from TMS mappings on motor and speech areas (Haddad et al., 2021; Lefaucheur and Picht, 2016). When delivering longer sequences of pulses, TMS can modulate the functioning of the brain and the effect can last beyond the stimulation session. This repetitive TMS (rTMS) has shown clinically relevant outcomes for example in depression and pain treatments and stroke rehabilitation (Lefaucheur et al., 2020). Even though not yet in clinical routine, TMS–EMG and TMS–EEG can be utilized as biomarkers to predict and follow the effects of TMS or other neuromodulatory and also pharmacological treatments (Cao et al., 2021; Ziemann et al., 2015).

4. Reliability of TMS

Even though there exist sophisticated methods to operate TMS and inspect its effects as introduced in the previous chapter, TMS methods are not error-free. In addition, variable ways to perform different parts of TMS protocols across laboratories and operators can lead to varying results. This chapter presents an overview of the factors related to the reliability of TMS. More detailed reviews are provided about two sources of variability (errors and differences in TMS navigation systems and varying approaches in selecting TMS parameters) that are relevant to all publications of this Thesis.

4.1 Terminology related to erroneousness

Accuracy, precision, repeatability, and reproducibility are terms that are sometimes utilized interchangeably despite being different concepts. According to the definitions by the International Organization for Standardization (ISO) and U.S. Food and Drug Administration (FDA), accuracy is specified as the nearness of ground truth and a measured value (FDA, 1995; ISO, 1994). The accuracy is often computed as the average difference between the ground truth and a series of measured values. To determine accuracy, the ground truth value, which can be an acknowledged reference value or a known true value, needs to be found out. Obtaining the ground truth can, however, be challenging. For example, in preoperative TMS mappings, DES has been utilized as a ground truth (Picht et al., 2013, 2011). However, DES requires opening the skull and is not necessarily more accurate than TMS.

Precision (also consistency or variability) is defined as a degree of scatter over repeated measurement results under certain conditions (FDA, 1995; ISO, 1994). Depending on the conditions, the precision becomes repeatability or reproducibility. Repeatability is variability over measurements performed by the same operator with the same device in the same laboratory with a short time between the measurements. Reproducibility describes the scatter of results collected when the operator, the device, and the laboratory are different. Precision measures are usually calculated as the standard deviation, variance, or coefficient of variation (the standard deviation divided by the mean) of the repeated measurements. Thus, precision-related measures represent random errors, and no information about the ground truth is needed. This sometimes leads to situations in which precision is reported as accuracy. Precision is often better than accuracy.

Accuracy and precision metrics derived from the definitions above were utilized in varying contexts in Publications 1, 2, and 4. In this Thesis, to cover all aspects of inaccuracy and variability, I use the general term reliability.

4.2 Factors affecting the reliability of TMS

Several factors can influence the variability of TMS results within a single session or multiple TMS sessions in the same or different laboratory. These factors can be classified, for example, into technical, methodological, operator-dependent, and subject-dependent components (see Fig. 4). I will give examples of these factors and how they affect MEP- and TEP-based measures in health. For example, Ridding and Ziemann (2010), Huang et al. (2017), and Guerra et al. (2020) have reviewed these factors from another perspective, i.e., how they affect rTMS-induced plasticity in health or disease.

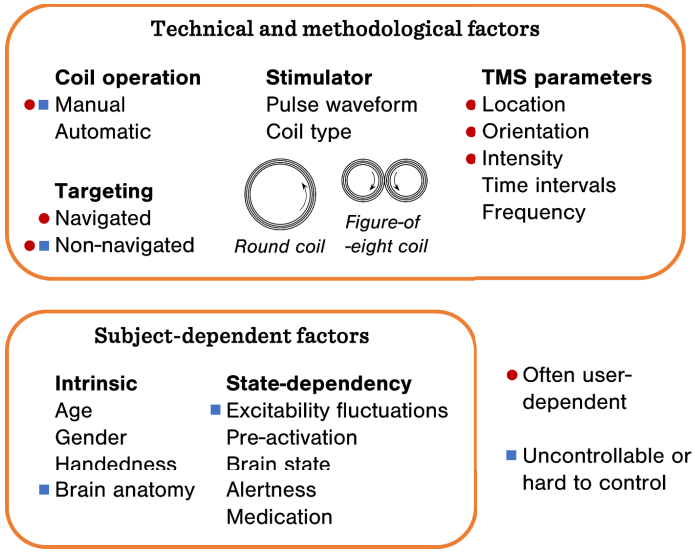

Figure 4. Factors that may influence the variability of TMS studies.

Technical factors affecting TMS variability are related to devices utilized for stimulation, navigation, and measuring TMS-evoked outcomes. There are different types of TMS coils, the most common being the figure-of-eight coil (see Fig. 4) inducing a focal E-field in the brain (Ueno et al., 1988). A round coil generates a wider and less specific E-field, and the variability of MEPs with a round coil has been reported lower as compared to the variability with a figure-of-eight coil (Kiers et al., 1993). The waveform of the current pulse fed into a TMS coil can vary across and within devices. The most typical pulse waveforms are monophasic (approximately half sinusoid) and biphasic (full sinusoid) forms, the latter resulting in lower MTs (Niehaus et al., 2000). Some devices can control the waveform in a flexible way (Gattinger et al., 2012; Koponen et al., 2018; Peterchev et al., 2014). The coil placement is often operated manually although more precise automatic methods exist

(see Section 5.1). The coil placement can be tracked and recorded with a neuronavigation system as introduced in Section 3.2. Differences and inaccuracies in TMS navigation systems are discussed more in detail in Section 4.3 and Publication 4. The TMS procedures can also be performed without navigation, at the cost of less stable MEPs (Cincotta et al., 2010; Julkunen et al., 2009), less reliable motor maps (Sondergaard et al., 2021), and even missing the intended spot due to lower targeting accuracy and precision. Technical factors also include devices that measure TMS responses. For example, artifacts occurring in TMS–EEG measurements may appear dissimilarly in different EEG devices due to alterations, e.g., in electrode and amplifier designs (Farzan et al., 2016; Ilmoniemi and Kičić, 2010; Rogasch et al., 2017).

Methodological factors that may vary across TMS studies are related to the measurement protocols. In these protocols, TMS parameters such as stimulation location, orientation, intensity, and timing between pulses play an important role. Even small changes in the location affect the amplitudes and latencies of MEPs (Kallioniemi et al., 2015; Koponen et al., 2018; Miranda et al., 1997; Publications 1 and 3) and TEP components (Casarotto et al., 2010; de Goede et al., 2018; Harquel et al., 2016; Rosanova et al., 2009). In addition, adjusting the orientation leads to altered MEP (Kallioniemi et al., 2015a; Souza et al., 2022; Publication 1) and TEP (Bonato et al., 2006; Casarotto et al., 2010; Publication 2) responses. When observing MEP amplitudes as a function of the stimulus intensity, the resulting relationship (input–output curve) resembles a sigmoidal function (Devanne et al., 1997). For TEPs, different stimulus intensities result in more complex changes (Komssi et al., 2004; Raffin et al., 2020). There exist a variety of approaches to select the TMS location, orientation, and intensity (see Section 4.4), and the procedures to determine these sensitive TMS parameters are often user-dependent and involve subjective decisions. Another important (but typically user-independent during a TMS session) TMS parameter is the timing between the consecutive pulses. A short millisecond-scale time interval between two stimuli can affect the amplitude of the resulting MEP as compared to an MEP of a single pulse. For example, if a TMS pulse is preceded by another sub-threshold pulse applied to the same location about 1–5 ms earlier, the MEP amplitude gets smaller (inhibition); if the time interval is 6–30 ms, the MEP amplitude increases (facilitation) (Kujirai et al., 1993; Ziemann et al., 1996). Previous pulses have been reported to affect MEPs even up to 5 s (Julkunen et al., 2012b) and 15 s (Hassanzahraee et al., 2019) time intervals.

Subject-dependent variability components can be divided, for example, into state-dependent and intrinsic factors. A significant state-dependent effect in motor cortex TMS is the variation of MEP amplitudes; even with fixed TMS settings, the MEP amplitude can vary by several millivolts. This deviation is thought to stem from excitability fluctuations in the corticospinal tract or desynchronization of spinal signals (Kiers et al., 1993; Magistris et al., 1998). Other state-dependent variability factors involve, for example, muscle pre-activation (lowers MT (Kiers et al., 1993)), drowsiness (increases MT (Avesani et al., 2008)), effects of medication (see, e.g., a review by Ziemann et al. (2015)), and phase of the ongoing EEG activity (Zrenner et al., 2018). The intrinsic aspects, which influence mainly inter-subject variability, include, e.g., age (Bashir et al., 2014; Pitcher et al., 2003), gender (Pitcher

et al., 2003), handedness (Triggs et al., 1999, 1994), and brain anatomy. Examples of important anatomical factors in TMS are the scalp-to-cortex distance, which affects the current strength needed in the coil (Herbsman et al., 2009; Julkunen et al., 2012a), and the individual folding of cortical structures together with unique anatomical connections between brain areas, which influence how the neurons are activated by TMS and how this activity spreads in the brain.

The list of factors affecting the variability of TMS outcomes is long and their effect on the total variability can be challenging to estimate. However, it is important to recognize them and especially the controllable factors that one could minimize to make TMS more effective and reliable.

4.3 Inaccuracies and variability in TMS navigation systems

Although outcomes with navigated TMS are reported to be more stable than with non-navigated coil placement (Bashir et al., 2011; Julkunen et al., 2009), also nTMS includes inaccuracies and variability. These are due to differences in the navigation methods over different systems as well as method- and operator-related errors in different steps of the navigation process. Error sources are listed in Table 1.

Table 1. Classification of errors related to TMS navigation systems. The scales of the errors are self-defined (minor, moderate, and major) based on the literature and the author's understanding of the error factor in question. The values for the effect of different error factors are often challenging to estimate.

	Navigation step	Error factor	Scale (and additional information)	References
Affects coil localization	Tool localization (head and coil trackers, digitizer tool)	Localization of a single navigation marker	Minor (sub-millimeters for optical tracking systems)	(Wiles et al., 2004)
		Arrangement of the marker groups	Minor (often in sub-millimeter scale, increases with distance from the marker set)	(Fitzpatrick et al., 1998)
		Angle between the marker group and the tracker camera	Minor (if the angle is smaller than 50°)	(West and Maurer Jr., 2004)
		Tolerances in manufacturing the trackers and the digitizer	Minor	(Ruohonen and Karhu, 2010)
	Registration of the coil to the coil model	Differences between the 3D model and the manufactured coil	Minor	(Hannula and Ilmoniemi, 2017)
		Tracker-to-physical coil registration (registration method, human error)	Minor (if calibrated by the manufacturer) to moderate (if the registration is done by the operator)	(Hannula and Ilmoniemi, 2017)

		Navigation step	Error factor		Scale (and additional information)	References
Affects coil localization		Head-to-MRI registration	Registration method (point-based or surface-based). Includes the effect of the number of points and their spatial distribution, and human error.		Moderate (with surface-based registration) to major (point-based registration, error increases further from the landmark points)	Publication 4
		Head tracking	Head tracker movement during TMS session		Can be major (up to several mm)	(Hannula and Ilmoniemi, 2017; Ruohonen and Karhu, 2010; Publication 4)
	Affects E-field computation	MRI	Deformations in MRI		Minor (if distortion correction applied and no metal present), otherwise can be major	(Maurer Jr et al., 2002; Torfeh et al., 2016)
			MRI voxel size		Minor (if the voxels small enough, e.g., ~1 mm^3)	(Hannula and Ilmoniemi, 2017; Ruohonen and Karhu, 2010)
			Segmentation method		Minor (with coil localization), moderate (with E-field computations)	(Nielsen et al., 2018; Rashed et al., 2021; Zaidi et al., 2021; Zhang et al., 2022)
			Utilizing MRI template instead of individual MRI		Can be major if not individually warped (with coil localization), major (with E-field computations)	(Fleischmann et al., 2020)
			Shifting of the brain between different postures		Minor	(Mikkonen and Laakso, 2019)
		Coil model	Manufacturing tolerances in coil windings		Minor	(Hannula and Ilmoniemi, 2017; Ruohonen and Karhu, 2010)
			Computational model of the coil		Minor to major	(Hannula and Ilmoniemi, 2017; Stenroos and Koponen, 2019)
		Head model	Geometry of the head model (spherical, realistic)		Minor to major	(Nummenmaa et al., 2013; Publication 4)
			Tissue conductivities		Moderate	(Saturnino et al., 2019)
		E-field model	Alternative methods	Line navigation	Can be major (especially with tilted coil placements)	(Hannula and Ilmoniemi, 2017; Sollmann et al., 2016)
				Analytical E-field computation with simple geometries	Moderate to major	(Nummenmaa et al., 2013; Publication 4)
				Numerical E-field computation with realistic models	Minor to major (depending on the head model)	(Stenroos and Koponen, 2019; Publication 4)

Errors related to nTMS are discussed also, for example, by Ruohonen and Karhu (2010), Hannula and Ilmoniemi (2017), and by Schönfeldt-Lecuona et al. (2005). A simulation analysis of the accuracy and precision of nTMS is presented in Publication 4. In addition, the literature from the field of neurosurgery navigation offers some useful information to the nTMS accuracy and precision (see, e.g., works by Fitzpatrick (2010), Maurer Jr et al. (2002), and Wang and Song (2011)). However, the exact methods in neurosurgery navigation are often different as compared to those of TMS navigation; thus, the information is not directly transferable to the TMS field. For example, in surgical applications, the accuracy of the head-to-MRI registration can be increased with implanted landmarks such as bone-attached screws (Mascott et al., 2006), which does not come into question in the non-invasive TMS field.

4.4 Determination of stimulation parameters

As mentioned earlier, there are various ways for targeting TMS, i.e., to determine the stimulation location, orientation, and intensity for TMS studies and treatments. The stimulation location is often determined by observing functional responses elicited by TMS. The most common feedback is a motor response when stimulating the primary motor cortex (M1). Typically, the selected stimulation location after a mapping is the one leading to the largest MEPs (Barker et al., 1985; Rossini et al., 2015). M1 targets of hand muscles have also been used as a reference for stimulation locations on other brain areas: for example, the dorsolateral prefrontal cortex (DLPFC; often utilized as a target for depression therapies) has been assumed to be situated about 5 cm (George et al., 1995; Pascual-Leone et al., 1996) anterior to the hand M1 target. However, this simple approach is rough and has been shown sub-optimal for targeting DLPFC (Cash et al., 2021; Trapp et al., 2020). Other functional responses that can be mapped to select stimulation locations are phosphenes or visual suppressions (Amassian et al., 1989; Meyer et al., 1991) and speech disruptions (Epstein et al., 1996; Lioumis et al., 2012; Pascual-Leone et al., 1991) when TMS is applied to occipital or speech areas, respectively. Methods for studying brain activity, such as EEG (Casarotto et al., 2022; Farzan et al., 2016; Tremblay et al., 2019), functional magnetic resonance imaging (Neggers et al., 2004; Sparing et al., 2008), or positron emission tomography (PET: Klirova et al., 2013; Plewnia et al., 2007), can also provide information about suitable stimulation locations. In addition, head anatomy can help in the selection process: for example, utilization of bony landmarks (Höflich et al., 1993; Mills et al., 1992) and EEG electrode positions (Beam et al., 2009; Herwig et al., 2003) have been reported. For taking into account individual brain anatomy, neuronavigation systems with subject-specific MRIs are of great help (Hannula and Ilmoniemi, 2017; Herwig et al., 2001; Ruohonen and Karhu, 2010). Instead of individual MRIs, neuronavigation and the selection of stimulation location are sometimes based on a brain template (Comeau, 2014; Fleischmann et al., 2020).

The stimulus orientation on the hand M1 is traditionally fixed to about 45° towards the midline from the posterior–anterior direction to have the stimulation approximately perpendicular to the wall of the precentral gyrus (Brasil-Neto et al., 1992; Mills et al., 1992). However, the anatomy of M1 and, thus, the optimal stimulation orientation varies across individuals (Balslev et al., 2007) and muscles (Bashir et al., 2013). Therefore, individualized determination of the stimulation orientation with the help of a neuronavigation system and MEP feedback is more meaningful. Selecting a stimulation orientation perpendicular to the gyral wall is suggested to be applicable also outside the motor cortex (Fox et al., 2004; Gomez-Tames et al., 2018; Janssen et al., 2015; Kammer et al., 2007).

The stimulus intensity is often set relative to the MT (Groppa et al., 2012; Rossini et al., 2015) or an intensity required for a certain average MEP amplitude (Rossini et al., 2015), regardless of the stimulated area. However, also MT can be defined in many ways (see a list of approaches, e.g., in the article by Groppa et al. (2012)). Moreover, it appears that the intensities determined based on MEPs are not directly transferable to other brain areas (Stewart et al., 2001; Tremblay et al., 2019). On other areas, MT-based stimulation intensity can be adjusted with the scalp-to-cortex distance (Knecht et al., 2005; Stokes et al., 2007) or one can utilize the estimated E-field magnitude in the cortex (Danner et al., 2012; Julkunen et al., 2012a). In addition, other functional measures, such as phosphenes (Stewart et al., 2001), TMS–PET (Siebner et al., 2003), and TMS–EEG responses (Casarotto et al., 2022; Komssi et al., 2004; Saari et al., 2018) have been suggested as feedback for adjusting the stimulation intensity.

Variability in selecting TMS parameters makes it challenging to interpret and compare observed effects in different TMS studies. It would be beneficial if the target selection was done more similarly. One meaningful and generalizable approach for TMS targeting is the already mentioned TMS–EEG approach, as it can provide direct neurophysiological feedback on all brain areas. TEP-based targeting has been applied for selecting stimulation parameters for TMS–EEG studies to ensure high-quality signals (Belardinelli et al., 2019; Casarotto et al., 2022, 2016). In addition, TMS–EEG has great potential as a functional targeting method for selecting the parameters for treatments and online guiding of therapeutic TMS. Publication 2 takes a step forward in TMS–EEG-based targeting by presenting and demonstrating an automatized set-up for optimizing TMS parameters with TEP feedback in an effortless way.

5. Automated TMS

One way to reduce operator-dependent differences in TMS procedures is to automate them. This requires a way to adjust TMS parameters non-manually and algorithms that make decisions on how the stimulation sequence is performed. In addition to increasing the reliability of TMS, automation can save time and make TMS sessions smoother. This chapter covers the elements needed for automating TMS processes (of which some were applied in Publications 1–3) and offers an overview of the existing automated procedures in the field of brain stimulation.

5.1 Automatic adjustment of stimulation parameters

An important element in automating TMS is the ability to automatically tune the stimulation parameters. The timing of the stimulation is simple to control with a triggering system that sends a pulse to the TMS device shortly before a stimulus is desired to be initiated. The stimulation intensity and orientation (180° flip) can be automatically tuned relatively easily by changing the amplitude and direction of the current fed to the TMS coil. Automatic adjustment of the stimulus location and orientation (with finer steps than 180°) requires more than simple current adjustment; traditionally TMS is operated with a single stimulation coil that is moved manually by the operator.

One way to bypass the human-hand-operated approach is to attach a TMS coil into a robotic arm (Lancaster et al., 2004; Lebossé et al., 2007; Noccaro et al., 2021; Yi and Bicker, 2010). Figure 5A shows an example of a TMS robot. Robotic control allows automatic adjustment of the coil position and orientation, enabling more reliable coil placement compared to manual coil operation (Ginhoux et al., 2013) and maintaining stable coil position by compensating head movements (Richter et al., 2013, 2010). However, planning the robotic movements can be challenging and access to some coil locations or orientations may be limited due to unsafe coil trajectories (Richter, 2013). The speed of coil movement is restricted, for example to about 1 cm/s (Grab et al., 2018) or 5 cm/s (Richter et al., 2010), due to safety limitations. TMS robots are commercially available.

Another approach is multi-channel TMS that takes one step forward by allowing adjustment of the stimulus location and orientation electronically, ultimately without a need for physical coil movements. This is achieved by operating several TMS coils concurrently (Ruohonen and Ilmoniemi, 1998). Tuning the relative amplitudes of currents flowing in the coils provides means to electronically change the E-field profile (sum of the E-fields of the individual coils, Fig. 5B), and thus the

stimulus location and orientation in the brain. A feasible implementation of such multi-channel TMS has been realized with tailored large planar overlapping coils (Koponen et al., 2018). Two coil versions of multi-locus TMS (mTMS) can either adjust the stimulus location on a one-dimensional line segment (Koponen et al., 2018; utilized in Publication 1) or the orientation (Souza et al., 2022; applied in Publications 1 and 2). A transducer consisting of five overlapping coils enables steering the stimulus location (in 2D) and orientation within a 3-cm-diameter cortical patch (Publication 3). Larger coverage of the cortex can be achieved, for example, by increasing the number of coils (Koponen et al., 2018; Nurmi et al., 2021). Other designs with small round coils on planar (Ruohonen and Ilmoniemi, 1998) or three-axis (Navarro de Lara et al., 2021) arrays have also been proposed. A clear advantage of multi-channel TMS is that, in principle, no time is needed for the parameter adjustments. This enables rapid stimulus sequences targeted to different locations with, for example, millisecond-scale time intervals (Nieminen et al., 2019) and faster compensation of small head movements compared to robots (Publication 3). Currently, multi-channel systems exist only as experimental devices and are not generally available.

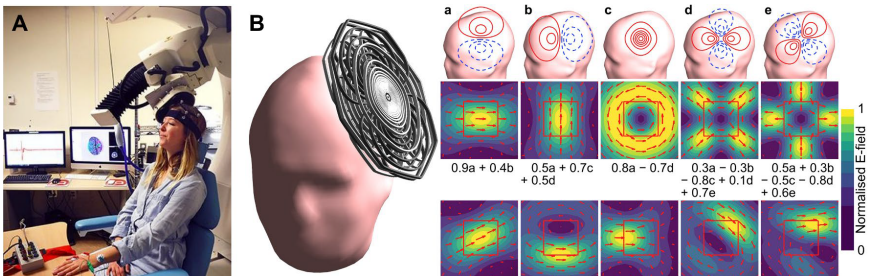

Figure 5. Example methods for automatic adjustment of stimulus location and orientation. **A**: Robotically controlled TMS. The photo is from an article by Grab et al. (2018) and reprinted with permission from Elsevier. **B**: Multi-locus TMS functions by summing the effects of individual overlapping coils (a–e, top row) with suitable weightings to adjust the location and orientation of the E-field maximum (yellow spots on the bottom row) within a defined region (red square). Illustration from Koponen et al. (2018), reprinted with permission from Elsevier.

5.2 Automated procedures in brain stimulation

Several TMS procedures have been automated with the help of the methods for adjusting TMS settings presented in the previous section. A stimulus sequence can be designed in advance and the automatic TMS system can be let to apply the desired pulses. Such a strategy has been implemented to scan automatically the motor areas by varying stimulus parameters with robotized (Ginhoux et al., 2013; Grab et al., 2018) or multi-locus (Koponen et al., 2018; Souza et al., 2022; Publications 1 and 3) TMS while measuring the evoked MEPs. Similar scanning is possible also on other parts of the cortex with TMS–EEG (Harquel et al., 2016; Publication 2).

The way TMS is delivered can be automatically adapted based on a recorded feedback signal in a so-called closed-loop manner. Examples of adaptive procedures in which stimulus intensity is varied and MEPs are utilized as feedback are the determination of motor threshold (Awiszus, 2003; Hassan et al., 2022) and the characterization of other properties of the MEP response curve (Alavi et al., 2021, 2019) with a minimal number of pulses. Another closed-loop procedure that has been automated is the finding of the stimulus location and orientation that maximizes MEP amplitudes (motor hotspot search) (Harquel et al., 2017; Meincke et al., 2016; Publication 1). Publication 2 presents a similar kind of procedure for finding optimal stimulation parameters with EEG responses as feedback. Moreover, EEG signals have been utilized in another type of automation in which the timing of the TMS pulse is aimed at a specific phase of the ongoing brain oscillations (Bergmann et al., 2012; Zrenner et al., 2018). This approach is considered as brain-state-dependent stimulation.

Automated procedures are of interest also with other brain-stimulation modalities. For example, Van Bueren et al. (2021) reported a closed-loop approach to optimize the frequency and intensity of transcranial alternating current stimulation (tACS) for better performance in a cognitive task, while Berényi et al. (2012) demonstrated switching on TES in a rodent model to suppress epileptic activity when it occurred. State-dependent and adaptive approaches have been applied also in DBS to trigger the stimulation when dysfunction-related brain activity is detected or tune the stimulation amplitude based on the feedback signal (Bouthour et al., 2019; Rosin et al., 2011).

5.3 Bayesian optimization with Gaussian processes

Many of the automation examples in the previous section include optimization, e.g., searching for a maximum (or a minimum) of a function. If we do not know the form of the function in advance, but we can get samples from it, the approach is called black-box optimization. One such example in the previous section was the search of TMS parameters that maximize the observed TMS-induced responses, for example, the amplitude of MEPs (Publication 1) or TEPs (Publication 2).

An analogous situation could happen on a far-off beach. Imagine that you have heard about a huge gold deposit under the ground along the 200-meter-long narrow beach (which can be considered as a 1D-line). In this case, you might be interested in finding the place where the gold deposit is closest to the ground, which would be an optimal place to start digging. You are prepared with a soil sampling drill that helps you to find out the distance to the gold deposit below the drilling site.

One way to find such an optimum is to take a soil sample from all locations on the beach. With this grid-search method, you would eventually find the best spot to dig the gold. It would, however, be laborious and time-consuming. Thus, it would be better to get the search done faster. There are solutions to make this kind of optimization in a clever and efficient way. An adequate approach for a problem like this is Bayesian optimization (for a review, see Shahriari et al., 2016) that helps to find the global optimum of an unknown function with a minimal number of samples even with noise present (the drilled depth samples in our example may be inaccurate).

Bayesian approaches are based on the idea that we often have in advance some know-how, although uncertain, about the problem in question. Due to uncertainty, the pieces of knowledge are treated as probabilities, and the probability distributions (infinite collection of potential outcomes) are updated once we get more information about the problem. For example, in the case of the gold-deposit example, we might know that the top of gold deposits in such an environment typically lies at around 5 m below the ground but may sometimes be only at 1 m depth. This prior information can be formed into so-called prior distribution when included in the Bayesian model.

Another piece needed in the Bayesian approach is the information about the data observations, i.e., how the data samples are like when everything else is fixed. For instance, the depth measurements of the gold can be inaccurate, but we can imagine an error margin of about ±1 m. This observation model is called likelihood. Multiplying these two probability distributions, the prior and the likelihood, together yields a posterior probability distribution updating our beliefs about the problem. In our gold-digging example, every time we get a new soil sample, our knowledge about the distribution of the gold deposit under the ground increases. With the Bayesian approach and the probability distributions in hand, we can take one step further and make predictions. In Bayesian optimization, we predict the value of the function of interest at the points that have not been sampled and forecast the future measurement values.

Bayesian optimization comprises two computation steps. The first step is to model the behavior of the unknown function (in the example case, the depth of the gold deposit along the beach) based on the data samples gathered (drilled soil samples). If the shape of the function is known in advance, one could employ parametric models. If the shape is unknown, it is better to use non-parametric models that assume no specific function shape, although the model itself may contain adjustable parameters. The most common non-parametric modeling approach in Bayesian optimization is called Gaussian process regression (Rasmussen and Williams, 2006) that we will apply also here. With Gaussian processes, the probability distributions are formed as a set of functions instead of distributions for individual variables. When modeling in this way, the set of possible functions that could represent our function to be modeled gets narrower once we get new data samples.

In Gaussian process regression, the prior distribution for function f to be modeled (e.g., the depth of the gold deposit under the ground) is $\mathbf{f} \sim \mathcal{N}(\boldsymbol{\mu}_0, \mathbf{K})$, which informs that the function values in a vector $\mathbf{f}$ follow a multivariate Gaussian distribution characterized by a mean function (vector $\boldsymbol{\mu}_0$) and a covariance function (matrix $\mathbf{K}$). If we have some idea about the shape of f in advance, that information can be included in prior mean $\boldsymbol{\mu}_0$. In our gold example, we knew the typical depth of the gold deposit, and the prior mean can be set to a constant function at 5 m depth. Another ingredient in the Gaussian process prior is the covariance function, which describes how much the values of f at different points ($\mathbf{x}_n$ and $\mathbf{x}_m$; note that $\mathbf{x}$ can also be a D-dimensional parameter vector) correlate. A typical choice for a covariance function is a squared exponential kernel

$$\mathbf{K}(n,m) = k(\mathbf{x}_n, \mathbf{x}_m) = a_0 \exp\left(-\sum_{d=1}^{D} a_{1,d}\left|x_{n,d} - x_{m,d}\right|^2\right), \tag{5.1}$$

in which the parameter a_0 tells how far the amplitudes of f can be from the prior mean $\boldsymbol{\mu}_0$, and a_1 regulates the smoothness of f. If a_1 is small, the function is smooth; if a_1 is large, f can oscillate more. D denotes the dimensions of the function, which was 1 in our example case as well as in Publications 1 and 2. This approach suits also for higher-dimensional problems, such as for optimizing TMS location in 2D domain. Other possibilities for kernel functions are listed, for example, by Shahriari et al. (2016) and Garnett (2022). The representation of the likelihood is more compact: as the measured data can contain errors, we set the likelihood model as $\mathbf{y} \sim \mathcal{N}(\mathbf{f}, \boldsymbol{\Lambda})$. The observed data samples $\mathbf{y}$ are independent and obey a normal distribution with variance λ^2 around the function values $\mathbf{f}$. $\boldsymbol{\Lambda}$ is a diagonal matrix with λ^2 values on its diagonal. A typical assumption is that the noise does not depend on the sampling parameters, i.e., the variance λ^2 is constant for all diagonal elements in $\boldsymbol{\Lambda}$. A changing variance could also be incorporated with another Gaussian process modeling the variance fluctuation (Frazier and Wang, 2016).

Both the prior and the likelihood distributions are Gaussian, and when combined, result in an analytical formula for the posterior distribution. With Gaussian process regression, we want to model f at all possible locations $\mathbf{x}$, meaning that we wish to make predictions about f at places elsewhere than the data sampling locations $\mathbf{X}$. This is possible by forming a posterior distribution, which after N data samples is

$$f(\mathbf{x}) \mid \mathbf{y}, \mathbf{X} \sim \mathcal{N}\left(\mu_N(\mathbf{x}), \sigma_N^2(\mathbf{x})\right), \tag{5.2}$$

where the so-called posterior mean (describing the most probable shape of f after observing data $\mathbf{y}$) is

$$\mu_N(\mathbf{x}) = \mu_0(\mathbf{x}) + \mathbf{k}(\mathbf{x}, \mathbf{X})(\mathbf{K} + \boldsymbol{\Lambda})^{-1}(\mathbf{y} - \boldsymbol{\mu}_0), \tag{5.3}$$

and the posterior variance expressing the uncertainty of the modeled f is defined as

$$\sigma_N^2(\mathbf{x}) = k(\mathbf{x}, \mathbf{x}) - \mathbf{k}(\mathbf{x}, \mathbf{X})(\mathbf{K} + \boldsymbol{\Lambda})^{-1}\mathbf{k}(\mathbf{x}, \mathbf{X})^{\mathrm{T}}. \tag{5.4}$$

The vector $\mathbf{k}(\mathbf{x}, \mathbf{X})$ includes the covariances between any location $\mathbf{x}$ and the measurement locations $\mathbf{X}$.

The second step in Bayesian optimization is adaptive data sampling, which means selecting the next sampling point so that the optimum is found with a minimal number of steps in the optimization process. In our gold example, this means that we would find the optimal spot for digging the gold as fast as possible. The guiding functions, which help in adaptive data sampling, are called acquisition functions, optimization policies, or infill criteria. Acquisition functions describe information gain that would be achieved when taking a sample at a given point, and they typically suggest sampling at points where the function to be optimized is possibly large (in maximization) due to posterior mean or uncertainty being high (Brochu et al., 2010;

Frazier and Wang, 2016). The next sampling point is where the acquisition function reaches its maximum. One example of an acquisition function is called knowledge gradient whose idea is to predict new data samples at each possible sampling location and estimate how much a new sample would change the maximum of the posterior mean (Frazier et al., 2009; Frazier and Wang, 2016). We selected the knowledge gradient as the guiding function in Publications 1 and 2, as it has been reported to perform well with noisy function evaluations (Picheny et al., 2013). Other acquisition functions are presented, e.g., by Shahriari et al. (2016) and Kochenderfer and Wheeler (2019).

The two steps in Bayesian optimization, modeling and adaptive data sampling, are repeated until the optimization process is considered ready, i.e., the maximum or minimum is found. The optimization can be stopped, for example, when a predefined number of samples has been reached or when the information gained from taking a new sample becomes small (Garnett, 2022). The stopping criteria are often tuned case-specifically. In our gold-digging example, we can stop taking soil samples if the estimate for the best digging location does not change with new samples or once we run out of time.

The optimization process with our gold deposit example is visualized in Fig. 6. After seeing this example, it is unsurprising that one of the first applications of the Gaussian processes was in mineral mining (Krige, 1951). Bayesian optimization with Gaussian processes has spread to a wide range of disciplines with other example applications in drug design (Sano et al., 2020) and tuning of hyperparameters for machine learning algorithms (Rasmussen and Williams, 2006). Bayesian optimization is well suited to automate optimizations performed in TMS procedures, as it tries to minimize the time needed and can deal with the unavoidable variation in electrophysiological responses that makes the optimization process challenging.

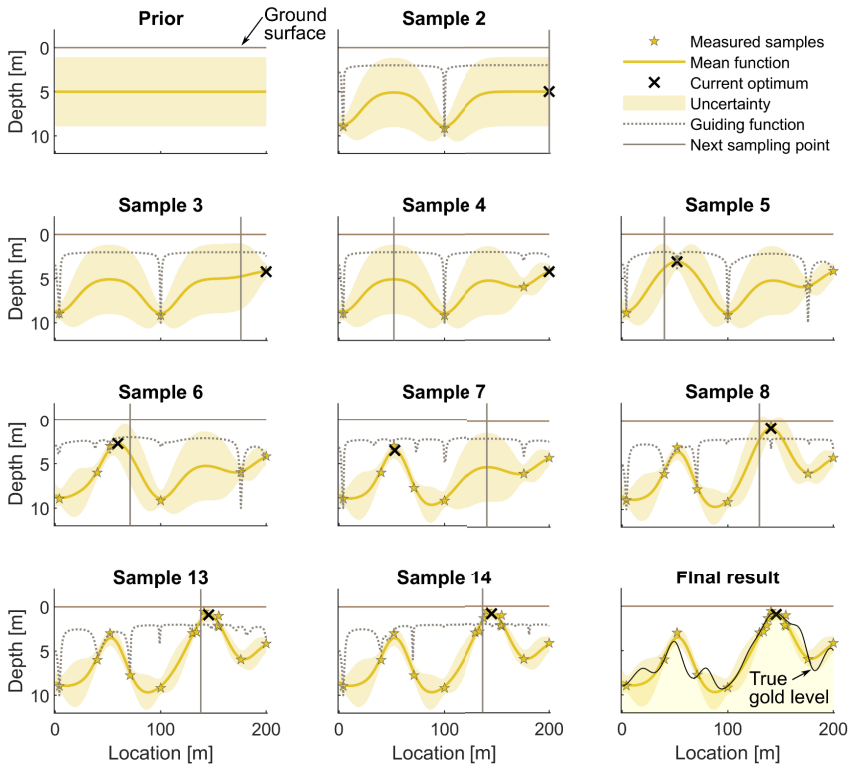

Figure 6. A gold mining example showing the procedure of Bayesian optimization with Gaussian processes. In the optimization process, the goal is to find the location where the gold deposit is closest to the surface of the ground. The first panel in the top left illustrates the starting point, in which the prior distribution has a constant prior mean at a depth of 5 m and a constant uncertainty interval. The following panels show the progress of the search with the measured soil samples marked as yellow stars, the posterior mean function as a yellow solid line, current optimum that is the maximum of the posterior mean function as a black cross, and the uncertainty represented with 95% credible interval (posterior mean ± 1.96 × √posterior variance) as a yellow shaded area. The gray dotted line is the knowledge-gradient guiding function, the maximum of which is the next sampling point (indicated as a vertical gray line). The last panel in the bottom right visualizes the search result after 15 soil samples: the best spot to start digging is marked as a black cross and the true depth of the gold deposit is shown as a black line.

6. Summary of publications

This chapter summarizes Publications 1–4.

6.1 Publication 1: Closed-loop TMS with motor responses

The aim of Publication 1 was to develop an algorithm for fast and automated search of stimulus parameters with MEPs as feedback. In the closed-loop setup (Fig. 7), stimulus parameters were controlled electronically with mTMS in 1D cases. In the first case, the location of the E-field maximum on a 3-cm-long line segment on the motor cortex was adjusted by utilizing a two-coil transducer comprising a figure-of-eight and an oval coil on the top of each other (Koponen et al., 2018). In the second case, the stimulus orientation on one location was tuned by two overlapping figure-of-eight coils (Souza et al., 2022). The evoked MEPs were recorded, and their peak-to-peak amplitudes were extracted online. Bayesian optimization and Gaussian processes (see Section 5.3) formed the mathematical basis for the algorithm. This approach helped to model the response curve as a function of the location or orientation based on the gathered MEPs. In addition, a guiding function suggested sampling points so that the search would converge with a minimal number of pulses.

The developed algorithm was tested on five subjects repeating the location and orientation searches 21 times. The results indicated that the closed-loop algorithm was able to optimize TMS parameters with good accuracy and precision. The average number of pulses needed in the searches was 17, corresponding to a search time of about 1.5 minutes.

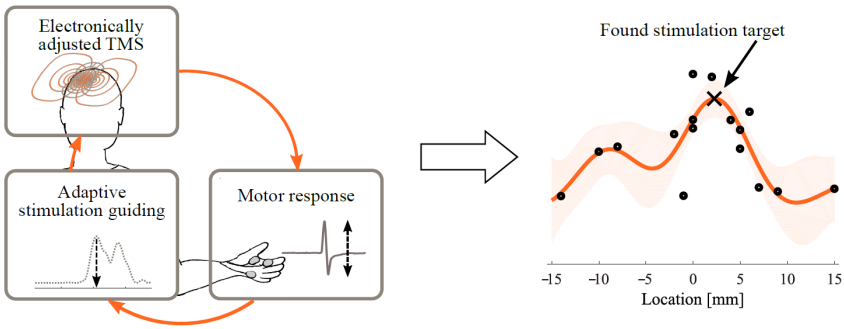

Figure 7. Flowchart of the motor-response-based optimization of TMS parameters (left) and an example result of an automated location search (right). The figure is from Publication 1 and reprinted with permission from Elsevier.

6.2 Publication 2: Closed-loop TMS with brain responses

Publication 2 aimed at performing similar kind of closed-loop optimization of TMS parameters as in Publication 1, but now with TEPs as feedback (see Fig. 8). For that, we first characterized the behaviour of TEPs as a function of the stimulus orientation because that was not known in advance. Systematic TEP mappings showed that the amplitudes of the early TEP deflections change with the stimulus orientation approximately in a sinusoidal way. Then, we applied the closed-loop algorithm to search the stimulus orientation that maximizes the peak-to-peak amplitude of the P20–N40 complex in the EEG response. The validation measurements were carried out with six subjects, repeating the orientation search 20 times. The average accuracy of the search outcomes was 13°, achieved with 40 pulses on average (corresponding to a search time of about 2 minutes).

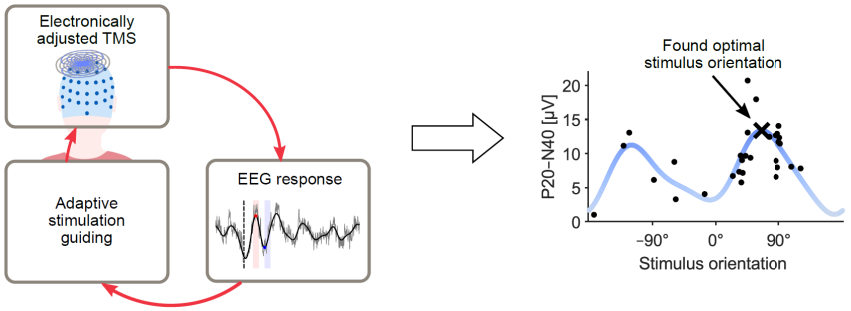

Figure 8. EEG-response-based target optimization. Flowchart of the closed-loop algorithm on the left, and an example outcome of the orientation optimization on the right. The figure is from Publication 2 and reprinted with permission from Elsevier.

6.3 Publication 3: Electronically targeted TMS

The goal of Publication 3 was to design, build, and characterize an mTMS system capable of electronically adjusting the stimulus location and orientation within a cortical patch. This was realized with a transducer consisting of five overlapping coils and connecting the individual coils into independently driven TMS circuits. In addition, Publication 3 presented an algorithm for electronic targeting, i.e., determining the relative currents fed to the coils so that the induced E-field maximum would be at the desired cortical location with the desired orientation.

From the point of view of this Thesis, the main outcome was the successful demonstration of the automated adjustment of TMS parameters in 3D (position and orientation of the E-field maximum) and the resulting motor maps of three separate muscles with one subject (Fig. 9). The 5-coil mTMS will allow a practical extension of the algorithms of Publication 1 and 2 into higher dimensions, i.e., optimizing the stimulus location and orientation at the same time.

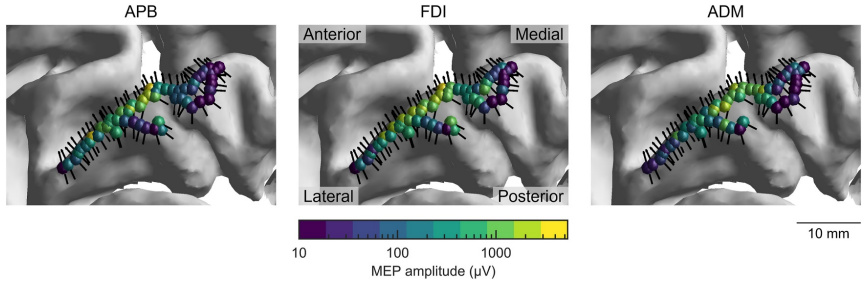

Figure 9. Motor maps obtained by steering the stimulus location and orientation with 5-coil mTMS. Motor maps of *abductor pollicis brevis* (APB), *first dorsal interosseus* (FDI), and *abductor digiti minimi* (ADM) muscles of the right hand in left, middle, and right panels, respectively. The figure is from Publication 3 and reprinted with permission from Elsevier.

6.4 Publication 4: Analysis of navigation errors

The aim of Publication 4 was to analyze the errors related to different methods used in TMS navigation systems. The analysis was done by computer simulations. The simulations showed that the largest contributors to the coregistration error were head-to-MRI registration and movement of the head tracker. There are two common ways, landmark- and surface-based approaches, to perform the head-to-MRI registration. The latter is clearly more reliable (see Fig. 10) and is thus the recommended option.

In addition, the simulations showed how the coregistration errors affect the E-field estimates computed with different approaches and varying levels of detail in the head model. When evaluated within E-field methods, the coregistration errors influenced the E-field estimates quite similarly across the E-field methods studied. When comparing the results against the most realistic E-field model applied, the accuracies generally enhanced with increasing level of detail in the E-field computation model. Thus, realistic E-field computations should be favored in navigation systems.

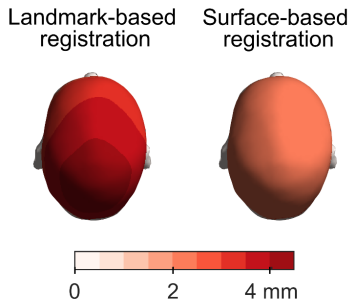

Figure 10. Scalp maps representing the total accuracy of coil positioning with neuronavigation systems relying on the landmark-based (left) or the surface-based (right) registration between the head and the MRI.

7. Discussion

This Thesis reviewed and analyzed errors and varying practices in TMS methods causing variability of results in the TMS field. In addition, this work contributed to reducing the variability and increasing the efficacy of TMS by presenting automated methods for TMS targeting and mapping. Next, I discuss the value of the results of this Thesis and suggest future directions in these topics.

7.1 Reliability of TMS targeting

As introduced earlier in this Thesis, navigation systems have an important role in reliable TMS targeting and mappings. The scale of nTMS accuracy and precision has been known to some extent. This Thesis (Publication 4) aimed at bringing more comprehensive information on the reliability of nTMS, for example, spatial distributions of different errors around the head, as the accuracy and precision estimates have typically been condensed into single average values.

The simulation analysis of Publication 4 revealed that, unsurprisingly, the main source of inaccuracy and imprecision in TMS coil navigation is the head-to-MRI registration, mainly due to human errors and MRI deformations. Based on the results, the recommendation is to apply surface-matching registration over landmark-based registration, as the first one leads to better coil-localization accuracy and precision. Moreover, one should be careful in MRI data acquisition (ear and scalp structures should not be squeezed by head supports) and perform the registration carefully. The second-largest source of error is the movement of the head tracker during the stimulation session. The operator needs to ensure that the tracker is kept fixed with respect to the subject's head; if the tracker moves, a new registration is required. Both of these error factors could be diminished with trackerless surface registration methods, such as laser scanning (Hironaga et al., 2019) or a structured-light approach (Olesen et al., 2010), although these methods need to become computationally more efficient to enable real-time tracking.

In addition to coil-localization errors, Publication 4 provided information on the accuracy and precision of the navigated E-field estimates on the cortex. The more realistic the E-field model, the better is the accuracy of the location, orientation, and magnitude of the tracked E-field maximum when compared to the most realistic model studied. The precision values are more even across the E-field computation models. Currently, commercial TMS navigation systems utilize simplified E-field estimation methods; however, applying more realistic methods also online

seems possible, for example, with recent developments in BEM-based E-field computations (Daneshzand et al., 2021; Stenroos and Koponen, 2019).

Navigated TMS is typically operated so that the coil is manually held or fixed to a coil holder. This way, it is impossible to keep the coil perfectly fixed with respect to the subject's head, as also the head can move. Thus, the navigation system may have tolerances of a few millimeters and degrees when helping to repeatedly trigger stimuli at the same spot with the same stimulus orientation. Even robotized TMS has limits for compensating head movements due to latency in initiating robot movements and because a constant small movement of the robot can be disturbing for the subject. In principle, mTMS (especially the version developed in Publication 3) could instantly adjust for these small movements with smaller tolerances enabling more accurate and precise stimulation with the desired TMS parameters. The verification of faster motion compensation with mTMS is a matter of future work.

Required navigation accuracy and precision levels are not clearly defined in the TMS field. Evidently, the accuracy requirements for nTMS are not as strict as in neurosurgery navigation, where millimeters can be a question of losing or preserving certain brain functions. However, high reliability of nTMS is of course often desired. For example, preoperative TMS mappings should be as accurate as possible so that the value of mapping is maximized (Lefaucheur and Picht, 2016). The precision of nTMS has a role in reliable targeting of treatments: if the treatment outcome is sensitive to the stimulus location, nTMS precision within and across sessions should be high. The impact of nTMS accuracy and precision in different applications needs to be studied more.

Even if the navigation were completely free of errors, TMS studies would still be accompanied by several sources of variability stemming from the subject and the operator as introduced in Sections 4.2 and 4.4. One variability factor mentioned was drowsiness, which can easily occur with an increasing length of the TMS session. Automated procedures can be considerably faster (Publications 1–3) than manual practice, reducing chances for the subject getting drowsy.

Another subject-dependent variability factor is the trial-to-trial variation of the electrophysiological responses such as MEPs and TEPs. To tackle MEP variability, one needs to acquire 20–30 responses with the same stimulus parameter for a reliable average (Biabani et al., 2018; Goldsworthy et al., 2016) or combine responses obtained with different stimulation parameters to a motor map with interpolation methods (Borghetti et al., 2008; Publication 1). Interestingly, MEPs are often considered highly variable and TEPs very repeatable and reliable even though the number of averaged TEPs is commonly 100–200. Information from a smaller number of TEPs with different stimulus parameters can also be interpolated into a map as demonstrated in Publication 2. To compare the effect of variability of MEPs and TEPs in the closed-loop optimizations, the MEP-based orientation search in Publication 1 reached an accuracy of about 10° with 15 MEPs on average, whereas the accuracy of the TEP-based orientation search in Publication 2 was approximately 20° with the same number of pulses. Thus, utilizing TEPs as a feedback signal needed more pulses for convergence. However, the search space was 360° and included two peaks in the underlying function in the TEP-based search. In the MEP-

based search, the search domain was 180° and the objective function had only one maximum.

The largest operator-dependent variability comes from the selection of TMS parameters. The ways to select TMS parameters are numerous, and these procedures often require many decisions by the operator. Therefore, it would be beneficial to apply proper automated protocols whenever possible, as the algorithms make the decisions with predefined logic, removing operator-dependent effects and increasing the reliability of TMS. Automated procedures presented in Publications 1 and 2 contribute to reducing operator dependency in the TMS field. However, this Thesis did not quantify the improvement of targeting reliability, thus, this aspect should be assessed in the future.

7.2 Closing the TMS loop

Closed-loop TMS with an electrophysiological feedback signal enables automated and effortless adjustment of TMS parameters. MEP-based target search had been demonstrated earlier (Harquel et al., 2017; Meincke et al., 2016), but the approach presented in Publication 1 is faster without compromising the accuracy. MEP-based searches are, however, limited to the motor cortex. Publication 2 demonstrated automated target search with TEPs, paving the way for targeting the stimulation with neurophysiological feedback all over the superficial cortex.

Targeting with neurophysiological feedback signals may circumvent some of the navigation errors analyzed in Publication 4, such as the co-registration errors. Even though the head-to-MRI registration would lead to varying co-registration results from session to session, one could rely on the feedback signal despite these navigation errors. If the head tracker moves during the TMS session, electrophysiological feedback signals could help in the readjustment process without re-registration when the same spot is targeted. On the other hand, such head-tracker movements would affect the reliability of MEP and TEP mapping results.

Future closed-loop targeting could employ anatomical information as a prior, for example, in defining the limits for the search space or selecting the initial sampling points. If the shape of the MEP- or TEP-based response function as a function of stimulus parameters at a given anatomical area is roughly known, this shape information could be incorporated in the prior model. These additions to the prior model could increase the accuracy and efficiency of automated searches. Another future step in the closed-loop searches would be to estimate the cortical location responsible for the observed response instead of just searching for the TMS parameters maximizing MEP or TEP features. This could be done by including the E-field information (Aonuma et al., 2018; Kataja et al., 2021; Opitz et al., 2013; Weise et al., 2020) and neuronal activation properties (Mutanen et al., 2021) into the process.

Automated closed-loop procedures require non-manual adjustment of TMS parameters. In Publications 1 and 2, we utilized mTMS, which is advantageous, as the electronic control of stimulus parameters does not necessitate physical coil movements. Closed-loop optimization could be performed with robotized TMS or by manually operated movements. However, mTMS is faster especially with EEG-based automatization because one does not need to wait for the stabilization of the

motion artifacts in the EEG signal, as would be required when the coil is moved between the pulses. Closed-loop algorithms in Publication 1 and 2 were demonstrated with 1D cases. However, the approach can be extended to several dimensions. Publication 3 successfully demonstrated automated motor mapping with predefined stimulus parameters by changing both the location and orientation of the peak E-field with the 5-coil mTMS system. Therefore, a natural next step with the presented closed-loop algorithms would be to make them work in several dimensions with the 5-coil mTMS system.

In addition, the ability for fast switching of stimulus parameters by mTMS enables investigating the dynamics of brain networks with time scales that are natural for neuronal information transmission. mTMS can deliver paired pulses or longer pulse sequences with different stimulus parameters with millisecond-scale time intervals enabling, for example, mapping of inhibitory or excitatory motor networks (Laine, 2021; Nieminen et al., 2019) or treating brain dysfunctions by coupling to multiple nodes of brain networks of interest instead of the traditional single-site treatments (Horn and Fox, 2020). Closed-loop algorithms presented in this Thesis can form a basis for performing such mappings or treatments in an automated way.

Despite the limited availability and need for further inventions regarding devices controlling spatial TMS parameters, technologies for the automation of TMS will continue to be developed. This is because there is an increasing interest in automating TMS procedures and treating brain dysfunctions in a closed-loop manner (Esposito et al., 2020; Farzan et al., 2016; Karabanov et al., 2016; Rotenberg, 2010; Zrenner et al., 2016). In the future, TMS interventions could be guided with online EEG feedback so that the sought plastic change is maximized. In addition, automation can increase the cost-effectiveness of clinical TMS.

When giving the control of TMS parameters to algorithms, I think that we should not blindly trust the algorithms. They are and will be of great help to the operator. However, there always needs to be somebody who follows the real-time functioning of the algorithms and checks that the result is meaningful. In addition, when letting algorithms guide therapies, one should also aim at gaining an understanding of the brain mechanisms behind the obtained effects. This would help in developing even more effective TMS therapies.

8. Conclusion

This Thesis recognizes that the reliability of TMS is affected, for example, by the methods applied, the decisions made by the operator, and biological variation that is unavoidable when dealing with a complex nervous system. Even though a substantial part of this Thesis discusses inaccuracies and variability in current TMS methods, the situation is not hopeless. Available sophisticated TMS methods enable adequate reliability, but the methods can still be improved, as shown in this work.

This Thesis suggests, for example, that the operator-dependent factors can be tackled by automating TMS procedures. Methods supporting TMS automation were presented in Publications 1–3. Automated algorithms can also be designed to cope with subject-dependent variability. The presented steps in automating TMS procedures increase the reliability of TMS, meeting the aim of this Thesis. Increased reliability of TMS can help to understand the functioning of the brain networks better as well as to develop more effective TMS treatments for neurological dysfunctions with the ultimate goal of improving patients' lives.

References

Aberra, A.S., Wang, B., Grill, W.M., Peterchev, A.V., 2020. Simulation of transcranial magnetic stimulation in head model with morphologically-realistic cortical neurons. Brain Stimul. 13, 175–189. https://doi.org/10.1016/j.brs.2019.10.002

Alavi, S.M.M., Goetz, S.M., Peterchev, A.V., 2019. Optimal estimation of neural recruitment curves using Fisher information: application to transcranial magnetic stimulation. IEEE Trans. Neural Syst. Rehabil. Eng. 27, 1320–1330. https://doi.org/10.1109/TNSRE.2019.2914475

Alavi, S.M.M., Goetz, S.M., Saif, M., 2021. Input–output slope curve estimation in neural stimulation based on optimal sampling principles. J. Neural Eng. 18, 046071. https://doi.org/10.1088/1741-2552/abffe5

Amassian, V.E., Cracco, R.Q., Maccabee, P.J., Cracco, J.B., 1992. Cerebello-frontal cortical projections in humans studied with the magnetic coil. Electroencephalogr. Clin. Neurophysiol. 85, 265–272. https://doi.org/10.1016/0168-5597(92)90115-R

Amassian, V.E., Cracco, R.Q., Maccabee, P.J., Cracco, J.B., Rudell, A., Eberle, L., 1989. Suppression of visual perception by magnetic coil stimulation of human occipital cortex. Electroencephalogr. Clin. Neurophysiol. 74, 458–462. https://doi.org/10.1016/0168-5597(89)90036-1

Aonuma, S., Gomez-Tames, J., Laakso, I., Hirata, A., Takakura, T., Tamura, M., Muragaki, Y., 2018. A high-resolution computational localization method for transcranial magnetic stimulation mapping. Neuroimage 172, 85–93. https://doi.org/10.1016/j.neuroimage.2018.01.039

Avesani, M., Formaggio, E., Fuggetta, G., Fiaschi, A., Manganotti, P., 2008. Corticospinal excitability in human subjects during nonrapid eye movement sleep: single and paired-pulse transcranial magnetic stimulation study. Exp. Brain Res. 187, 17–23. https://doi.org/10.1007/s00221-008-1274-3

Awiszus, F., 2003. TMS and threshold hunting. Suppl. Clin. Neurophysiol. 56, 13–23. https://doi.org/10.1016/S1567-424X(09)70205-3

Baker, S.N., Olivier, E., Lemon, R.N., 1995. Task-related variation in corticospinal output evoked by transcranial magnetic stimulation in the macaque monkey. J. Physiol. 488, 795–801. https://doi.org/10.1113/jphysiol.1995.sp021011

Balslev, D., Braet, W., McAllister, C., Miall, R.C., 2007. Inter-individual variability in optimal current direction for transcranial magnetic stimulation of the motor cortex. J. Neurosci. Methods 162, 309–313. https://doi.org/10.1016/j.jneumeth.2007.01.021

Barker, A.T., Jalinous, R., Freeston, I.L., 1985. Non-invasive magnetic stimulation of human motor cortex. Lancet 325, 1106–1107. https://doi.org/10.1016/S0140-6736(85)92413-4

Bashir, S., Edwards, D., Pascual-Leone, A., 2011. Neuronavigation increases the physiologic and behavioral effects of low-frequency rTMS of primary motor cortex in healthy subjects. Brain Topogr. 24, 54–64. https://doi.org/10.1007/s10548-010-0165-7

Bashir, S., Perez, J.M., Horvath, J.C., Pascual-Leone, A., 2013. Differentiation of motor cortical representation of hand muscles by navigated mapping of optimal TMS current directions in healthy subjects. J. Clin. Neurophysiol. 30, 390–395. https://doi.org/10.1097/WNP.0b013e31829dda6b

Bashir, S., Perez, J.M., Horvath, J.C., Pena-Gomez, C., Vernet, M., Capia, A., Alonso-Alonso, M., Pascual-Leone, A., 2014. Differential effects of motor cortical excitability and plasticity in young and old individuals: a transcranial magnetic stimulation (TMS) study. Front. Aging Neurosci. 6, 111. https://doi.org/10.3389/fnagi.2014.00111

Beam, W., Borckardt, J.J., Reeves, S.T., George, M.S., 2009. An efficient and accurate new method for locating the F3 position for prefrontal TMS applications. Brain Stimul. 2, 50–54. https://doi.org/10.1016/j.brs.2008.09.006

Belardinelli, P., Biabani, M., Blumberger, D.M., Bortoletto, M., Casarotto, S., David, O., Desideri, D., Etkin, A., Ferrarelli, F., Fitzgerald, P.B., Fornito, A., Gordon, P.C., Gosseries, O., Harquel, S., Julkunen, P., Keller, C.J., Kimiskidis, V.K., Lioumis, P., Miniussi, C., Rosanova, M., Rossi, S., Sarasso, S., Wu, W., Zrenner, C., Daskalakis, Z.J., Rogasch, N.C., Massimini, M., Ziemann, U., Ilmoniemi, R.J., 2019. Reproducibility in TMS–EEG studies: a call for data sharing, standard procedures and effective experimental control. Brain Stimul. 12, 787–790. https://doi.org/10.1016/j.brs.2019.01.010

Berényi, A., Belluscio, M., Mao, D., Buzsáki, G., 2012. Closed-loop control of epilepsy by transcranial electrical stimulation. Science 337, 735–737. https://doi.org/10.1126/science.1223154

Bergmann, T.O., Mölle, M., Schmidt, M.A., Lindner, C., Marshall, L., Born, J., Siebner, H.R., 2012. EEG-guided transcranial magnetic stimulation reveals rapid shifts in motor cortical excitability during the human sleep slow oscillation. J. Neurosci. 32, 243–253. https://doi.org/10.1523/JNEUROSCI.4792-11.2012

Biabani, M., Farrell, M., Zoghi, M., Egan, G., Jaberzadeh, S., 2018. The minimal number of TMS trials required for the reliable assessment of corticospinal excitability, short interval intracortical inhibition, and intracortical facilitation. Neurosci. Lett. 674, 94–100. https://doi.org/10.1016/j.neulet.2018.03.026

Bonato, C., Miniussi, C., Rossini, P.M., 2006. Transcranial magnetic stimulation and cortical evoked potentials: a TMS/EEG co-registration study. Clin. Neurophysiol. 117, 1699–1707. https://doi.org/10.1016/j.clinph.2006.05.006

Borghetti, D., Sartucci, F., Petacchi, E., Guzzetta, A., Piras, M.F., Murri, L., Cioni, G., 2008. Transcranial magnetic stimulation mapping: a model based on spline interpolation. Brain Res. Bull. 77, 143–148. https://doi.org/10.1016/j.brainresbull.2008.06.001

Bouthour, W., Mégevand, P., Donoghue, J., Lüscher, C., Birbaumer, N., Krack, P., 2019. Biomarkers for closed-loop deep brain stimulation in Parkinson disease and beyond. Nat. Rev. Neurol. 15, 343–352. https://doi.org/10.1038/s41582-019-0166-4

Brasil-Neto, J.P., Cohen, L.G., Panizza, M., Nilsson, J., Roth, B.J., Hallett, M., 1992. Optimal focal transcranial magnetic activation of the human motor cortex: effects of coil orientation, shape of the induced current pulse, and stimulus intensity. J. Clin. Neurophysiol. 9, 132–136. https://doi.org/10.1097/00004691-199201000-00014

Brochu, E., Cora, V.M., de Freitas, N., 2010. A tutorial on Bayesian optimization of expensive cost functions, with application to active user modeling and hierarchical reinforcement learning. arXiv 1012.2599.

Cao, K.-X., Ma, M.-L., Wang, C.-Z., Iqbal, J., Si, J.-J., Xue, Y.-X., Yang, J.-L., 2021. TMS-EEG: an emerging tool to study the neurophysiologic biomarkers of psychiatric disorders. Neuropharmacology 197, 108574. https://doi.org/10.1016/j.neuropharm.2021.108574

Casarotto, S., Comanducci, A., Rosanova, M., Sarasso, S., Fecchio, M., Napolitani, M., Pigorini, A., Casali, A.G., Trimarchi, P.D., Boly, M., Gosseries, O., Bodart, O., Curto, F., Landi, C., Mariotti, M., Devalle, G., Laureys, S., Tononi, G., Massimini, M., 2016. Stratification of unresponsive patients by an independently validated index of brain complexity. Ann. Neurol. 80, 718–729. https://doi.org/10.1002/ana.24779

Casarotto, S., Fecchio, M., Rosanova, M., Varone, G., D'Ambrosio, S., Sarasso, S., Pigorini, A., Russo, S., Comanducci, A., Ilmoniemi, R.J., Massimini, M., 2022. The rt-TEP tool: real-time visualization of TMS-evoked potential to maximize cortical activation and minimize artifacts. J. Neurosci. Methods 370, 109486. https://doi.org/10.1016/j.jneumeth.2022.109486

Casarotto, S., Romero Lauro, L.J., Bellina, V., Casali, A.G., Rosanova, M., Pigorini, A., Defendi, S., Mariotti, M., Massimini, M., 2010. EEG responses to TMS are sensitive to changes in the perturbation parameters and repeatable over time. PLoS One 5, e10281. https://doi.org/10.1371/journal.pone.0010281

Cash, R.F.H., Weigand, A., Zalesky, A., Siddiqi, S.H., Downar, J., Fitzgerald, P.B., Fox, M.D., 2021. Using brain imaging to improve spatial targeting of transcranial magnetic stimulation for depression. Biol. Psychiatry 90, 689–700. https://doi.org/10.1016/j.biopsych.2020.05.033

Cincotta, M., Giovannelli, F., Borgheresi, A., Balestrieri, F., Toscani, L., Zaccara, G., Carducci, F., Viggiano, M.P., Rossi, S., 2010. Optically tracked neuronavigation increases the stability of hand-held focal coil positioning: evidence from "transcranial" magnetic stimulation-induced electrical field measurements. Brain Stimul. 3, 119–123. https://doi.org/10.1016/j.brs.2010.01.001

Comeau, R., 2014. Neuronavigation for transcranial magnetic stimulation, in: Rotenberg, A., Horvath, J.C., Pascual-Leone, A. (Eds.), Transcranial Magnetic Stimulation. Humana Press, New York, pp. 31–56. https://doi.org/10.1007/978-1-4939-0879-0_3

Cracco, R.Q., Amassian, V.E., Maccabee, P.J., Cracco, J.B., 1989. Comparison of human transcallosal responses evoked by magnetic coil and electrical stimulation. Electroencephalogr. Clin. Neurophysiol. 74, 417–427. https://doi.org/10.1016/0168-5597(89)90030-0

Daneshzand, M., Makarov, S.N., Navarro de Lara, L.I., Guerin, B., McNab, J., Rosen, B.R., Hämäläinen, M.S., Raij, T., Nummenmaa, A., 2021. Rapid computation of TMS-induced E-fields using a dipole-based magnetic stimulation profile approach. Neuroimage 237, 118097. https://doi.org/10.1016/j.neuroimage.2021.118097

Danner, N., Könönen, M., Säisänen, L., Laitinen, R., Mervaala, E., Julkunen, P., 2012. Effect of individual anatomy on resting motor threshold – computed electric field as a measure of cortical excitability. J. Neurosci. Methods 203, 298–304. https://doi.org/10.1016/j.jneumeth.2011.10.004

de Goede, A.A., ter Braack, E.M., van Putten, M.J.A.M., 2018. Accurate coil positioning is important for single and paired pulse TMS on the subject level. Brain Topogr. 31, 917–930. https://doi.org/10.1007/s10548-018-0655-6

Devanne, H., Lavoie, B.A., Capaday, C., 1997. Input-output properties and gain changes in the human corticospinal pathway. Exp. Brain Res. 114, 329–338. https://doi.org/10.1007/PL00005641

Di Lazzaro, V., 2013. Biological effects of non-invasive brain stimulation. Handb. Clin. Neurol. 116, 367–374. https://doi.org/10.1016/B978-0-444-53497-2.00030-9

Di Lazzaro, V., Oliviero, A., Pilato, F., Saturno, E., Dileone, M., Mazzone, P., Insola, A., Tonali, P.A., Rothwell, J.C., 2004. The physiological basis of transcranial motor cortex stimulation in conscious humans. Clin. Neurophysiol. 115, 255–266. https://doi.org/10.1016/j.clinph.2003.10.009

Epstein, C.M., Lah, J.J., Meador, K., Weissman, J.D., Gaitan, L.E., Dihenia, B., 1996. Optimum stimulus parameters for lateralized suppression of speech with magnetic brain stimulation. Neurology 47, 1590–1593. https://doi.org/10.1212/WNL.47.6.1590

Esposito, R., Bortoletto, M., Miniussi, C., 2020. Integrating TMS, EEG, and MRI as an approach for studying brain connectivity. Neuroscientist 26, 471–486. https://doi.org/10.1177/1073858420916452

Farzan, F., Vernet, M., Shafi, M.M.D., Rotenberg, A., Daskalakis, Z.J., Pascual-Leone, A., 2016. Characterizing and modulating brain circuitry through transcranial magnetic stimulation combined with electroencephalography. Front. Neural Circuits 10, 73. https://doi.org/10.3389/fncir.2016.00073

FDA, 1995. Guideline for Industry: Text on Validation of Analytical Procedures. U. S. Food and Drug Administration/Center for Biologics Evaluation and Research 1–9.

Fitzpatrick, J.M., 2010. The role of registration in accurate surgical guidance. Proc. Inst. Mech. Eng. Part H J. Eng. Med. 224, 607–622. https://doi.org/10.1243/09544119JEIM589

Fitzpatrick, J.M., West, J.B., Maurer, C.R., 1998. Predicting error in rigid-body point-based registration. IEEE Trans. Med. Imaging 17, 694–702. https://doi.org/10.1109/42.736021

Fleischmann, R., Köhn, A., Tränkner, S., Brandt, S.A., Schmidt, S., 2020. Individualized template MRI is a valid and reliable alternative to individual MRI for spatial tracking in navigated TMS studies in healthy subjects. Front. Hum. Neurosci. 14, 174. https://doi.org/10.3389/fnhum.2020.00174

Fox, P.T., Narayana, S., Tandon, N., Sandoval, H., Fox, S.P., Kochunov, P., Lancaster, J.L., 2004. Column-based model of electric field excitation of cerebral cortex. Hum. Brain Mapp. 22, 1–14. https://doi.org/10.1002/hbm.20006

Frazier, P., Powell, W., Dayanik, S., 2009. The knowledge-gradient policy for correlated normal beliefs. INFORMS J. Comput. 21, 599–613. https://doi.org/10.1287/ijoc.1080.0314

Frazier, P.I., Wang, J., 2016. Bayesian optimization for materials design, in: Lookman, T., Alexander, F.J., Rajan, K. (Eds.), Information Science for Materials Discovery and Design. Springer, Cham, pp. 45–75. https://doi.org/10.1007/978-3-319-23871-5_3

Garnett, R., 2022. Bayesian Optimization. https://bayesoptbook.com/.

Gattinger, N., Moessnang, G., Gleich, B., 2012. flexTMS—a novel repetitive transcranial magnetic stimulation device with freely programmable stimulus currents. IEEE Trans. Biomed. Eng. 59, 1962–1970. https://doi.org/10.1109/TBME.2012.2195180

George, M.S., Wassermann, E.M., Williams, W.A., Callahan, A., Ketter, T.A., Basser, P., Hallett, M., Post, R.M., 1995. Daily repetitive transcranial magnetic stimulation (rTMS) improves mood in depression. Neuroreport 6, 1853–1856. https://doi.org/10.1097/00001756-199510020-00008

Ginhoux, R., Renaud, P., Zorn, L., Goffin, L., Bayle, B., Foucher, J., Lamy, J., Armspach, J.P., De Mathelin, M., 2013. A custom robot for transcranial magnetic stimulation: first assessment on healthy subjects. Proc. Annu. Int. Conf. IEEE Eng. Med. Biol. Soc. 5352–5355. https://doi.org/10.1109/EMBC.2013.6610758

Goldsworthy, M.R., Hordacre, B., Ridding, M.C., 2016. Minimum number of trials required for within- and between-session reliability of TMS measures of corticospinal excitability. Neuroscience 320, 205–209. https://doi.org/10.1016/j.neuroscience.2016.02.012

Gomez-Tames, J., Hamasaka, A., Laakso, I., Hirata, A., Ugawa, Y., 2018. Atlas of optimal coil orientation and position for TMS: a computational study. Brain Stimul. 11, 839–848. https://doi.org/10.1016/j.brs.2018.04.011

Grab, J.G., Zewdie, E., Carlson, H.L., Kuo, H.-C., Ciechanski, P., Hodge, J., Giuffre, A., Kirton, A., 2018. Robotic TMS mapping of motor cortex in the developing brain. J. Neurosci. Methods 309, 41–54. https://doi.org/10.1016/j.jneumeth.2018.08.007

Groppa, S., Oliviero, A., Eisen, A., Quartarone, A., Cohen, L.G., Mall, V., Kaelin-Lang, A., Mima, T., Rossi, S., Thickbroom, G.W., Rossini, P.M., Ziemann, U., Valls-Solé, J., Siebner, H.R., 2012. A practical guide to diagnostic transcranial magnetic stimulation: report of an IFCN committee. Clin. Neurophysiol. 123, 858–882. https://doi.org/10.1016/j.clinph.2012.01.010

Guerra, A., López-Alonso, V., Cheeran, B., Suppa, A., 2020. Variability in non-invasive brain stimulation studies: reasons and results. Neurosci. Lett. 719, 133330. https://doi.org/10.1016/j.neulet.2017.12.058

Haddad, A.F., Young, J.S., Berger, M.S., Tarapore, P.E., 2021. Preoperative applications of navigated transcranial magnetic stimulation. Front. Neurol. 11, 628903. https://doi.org/10.3389/fneur.2020.628903

Hannula, H., Ilmoniemi, R.J., 2017. Basic principles of navigated TMS, in: Krieg, S.M. (Ed.), Navigated Transcranial Magnetic Stimulation in Neurosurgery. Springer, Cham, pp. 3–29.

Harquel, S., Bacle, T., Beynel, L., Marendaz, C., Chauvin, A., David, O., 2016. Mapping dynamical properties of cortical microcircuits using robotized TMS and EEG: towards functional cytoarchitectonics. Neuroimage 135, 115–124. https://doi.org/10.1016/j.neuroimage.2016.05.009

Harquel, S., Diard, J., Raffin, E., Passera, B., Dall'Igna, G., Marendaz, C., David, O., Chauvin, A., 2017. Automatized set-up procedure for transcranial magnetic stimulation protocols. Neuroimage 153, 307–318. https://doi.org/10.1016/j.neuroimage.2017.04.001

Hassan, U., Pillen, S., Zrenner, C., Bergmann, T.O., 2022. The brain electrophysiological recording & stimulation (BEST) toolbox. Brain Stimul. 15, 109–115. https://doi.org/10.1016/j.brs.2021.11.017

Hassanzahraee, M., Zoghi, M., Jaberzadeh, S., 2019. Longer transcranial magnetic stimulation intertrial interval increases size, reduces variability, and improves the reliability of motor evoked potentials. Brain Connect. 9, 770–776. https://doi.org/10.1089/brain.2019.0714

Heller, L., van Hulsteyn, D.B., 1992. Brain stimulation using electromagnetic sources: theoretical aspects. Biophys. J. 63, 129–138. https://doi.org/10.1016/S0006-3495(92)81587-4

Herbsman, T., Forster, L., Molnar, C., Dougherty, R., Christie, D., Koola, J., Ramsey, D., Morgan, P.S., Bohning, D.E., George, M.S., Nahas, Z., 2009. Motor threshold in transcranial magnetic stimulation: the impact of white matter fiber orientation and skull-to-cortex distance. Hum. Brain Mapp. 30, 2044–2055. https://doi.org/10.1002/hbm.20649

Herwig, U., Satrapi, P., Schönfeldt-Lecuona, C., 2003. Using the international 10-20 EEG system for positioning of transcranial magnetic stimulation. Brain Topogr. 16, 95–99. https://doi.org/10.1023/B:BRAT.0000006333.93597.9d

Herwig, U., Schönfeldt-Lecuona, C., Wunderlich, A.P., von Tiesenhausen, C., Thielscher, A., Walter, H., Spitzer, M., 2001. The navigation of transcranial magnetic stimulation. Psychiatry Res. Neuroimaging 108, 123–31. https://doi.org/10.1016/S0925-4927(01)00121-4

Hironaga, N., Kimura, T., Mitsudo, T., Gunji, A., Iwata, M., 2019. Proposal for an accurate TMS-MRI co-registration process via 3D laser scanning. Neurosci. Res. 144, 30–39. https://doi.org/10.1016/j.neures.2018.08.012

Höflich, G., Kasper, S., Hufnagel, A., Ruhrmann, S., Möller, H.-J., 1993. Application of transcranial magnetic stimulation in treatment of drug-resistant major depression—a report of two cases. Hum. Psychopharmacol. Clin. Exp. 8, 361–365. https://doi.org/10.1002/hup.470080510

Horn, A., Fox, M.D., 2020. Opportunities of connectomic neuromodulation. Neuroimage 221, 117180. https://doi.org/10.1016/j.neuroimage.2020.117180

Huang, Y.-Z., Lu, M.-K., Antal, A., Classen, J., Nitsche, M., Ziemann, U., Ridding, M., Hamada, M., Ugawa, Y., Jaberzadeh, S., Suppa, A., Paulus, W., Rothwell, J., 2017. Plasticity induced by non-invasive transcranial brain stimulation: a position paper. Clin. Neurophysiol. 128, 2318–2329. https://doi.org/10.1016/j.clinph.2017.09.007

Ilmoniemi, R.J., Hernandez-Pavon, J.C., Mäkelä, N.N., Metsomaa, J., Mutanen, T.P., Stenroos, M., Sarvas, J., 2015. Dealing with artifacts in TMS-evoked EEG. Proc. Annu. Int. Conf. IEEE Eng. Med. Biol. Soc. 230–233. https://doi.org/10.1109/EMBC.2015.7318342

Ilmoniemi, R.J., Kičić, D., 2010. Methodology for combined TMS and EEG. Brain Topogr. 22, 233–248. https://doi.org/10.1007/s10548-009-0123-4

Ilmoniemi, R.J., Ruohonen, J., Karhu, J., 1999. Transcranial magnetic stimulation — a new tool for functional imaging of the brain. Crit. Rev. Biomed. Eng. 27, 241–284.

Ilmoniemi, R.J., Sarvas, J., 2019. Brain Signals, Physics and Mathematics of MEG and EEG. The MIT Press, Cambridge.

Ilmoniemi, R.J., Virtanen, J., Ruohonen, J., Karhu, J., Aronen, H.J., Näätänen, R., Katila, T., 1997. Neuronal responses to magnetic stimulation reveal cortical reactivity and connectivity. Neuroreport 8, 3537–3540. https://doi.org/10.1097/00001756-199711100-00024

ISO, 1994. ISO 5725-1: Accuracy (trueness and precision) of measurement methods and results — Part 1: general principles and definitions. International Organization for Standardization.

Janssen, A.M., Oostendorp, T.F., Stegeman, D.F., 2015. The coil orientation dependency of the electric field induced by TMS for M1 and other brain areas. J. Neuroeng. Rehabil. 12, 47. https://doi.org/10.1186/s12984-015-0036-2

Julkunen, P., Säisänen, L., Danner, N., Awiszus, F., Könönen, M., 2012a. Within-subject effect of coil-to-cortex distance on cortical electric field threshold and motor evoked potentials in transcranial magnetic stimulation. J. Neurosci. Methods 206, 158–164. https://doi.org/10.1016/j.jneumeth.2012.02.020

Julkunen, P., Säisänen, L., Danner, N., Niskanen, E., Hukkanen, T., Mervaala, E., Könönen, M., 2009. Comparison of navigated and non-navigated transcranial magnetic stimulation for motor cortex mapping, motor threshold and motor evoked potentials. Neuroimage 44, 790–795. https://doi.org/10.1016/j.neuroimage.2008.09.040

Julkunen, P., Säisänen, L., Hukkanen, T., Danner, N., Könönen, M., 2012b. Does second-scale intertrial interval affect motor evoked potentials induced by single-pulse transcranial magnetic stimulation? Brain Stimul. 5, 526–532. https://doi.org/10.1016/j.brs.2011.07.006

Kallioniemi, E., Könönen, M., Säisänen, L., Gröhn, H., Julkunen, P., 2015a. Functional neuronal anisotropy assessed with neuronavigated transcranial magnetic stimulation. J. Neurosci. Methods 256, 82–90. https://doi.org/10.1016/j.jneumeth.2015.08.028

Kallioniemi, E., Pitkänen, M., Säisänen, L., Julkunen, P., 2015b. Onset latency of motor evoked potentials in motor cortical mapping with neuronavigated transcranial magnetic stimulation. Open Neurol. J. 9, 62–69. https://doi.org/10.2174/1874205x01509010062

Kammer, T., Vorwerg, M., Herrnberger, B., 2007. Anisotropy in the visual cortex investigated by neuronavigated transcranial magnetic stimulation. Neuroimage 36, 313–321. https://doi.org/10.1016/j.neuroimage.2007.03.001

Karabanov, A., Thielscher, A., Siebner, H.R., 2016. Transcranial brain stimulation: closing the loop between brain and stimulation. Curr. Opin. Neurol. 29, 397–404. https://doi.org/10.1097/WCO.0000000000000342

Kataja, J., Soldati, M., Matilainen, N., Laakso, I., 2021. A probabilistic transcranial magnetic stimulation localization method. J. Neural Eng. 18, 0460f3. https://doi.org/10.1088/1741-2552/ac1f2b

Kiers, L., Cros, D., Chiappa, K.H., Fang, J., 1993. Variability of motor potentials evoked by transcranial magnetic stimulation. Electroencephalogr. Clin. Neurophysiol. 89, 415–423. https://doi.org/https://doi.org/10.1016/0168-5597(93)90115-6

Kirschstein, T., Köhling, R., 2009. What is the source of the EEG? Clin. EEG Neurosci. 40, 146–149. https://doi.org/10.1177/155005940904000305

Klirova, M., Horacek, J., Novak, T., Cermak, J., Spaniel, F., Skrdlantova, L., Mohr, P., Höschl, C., 2013. Individualized rTMS neuronavigated according to regional brain metabolism (18FGD PET) has better treatment effects on auditory hallucinations than standard positioning of rTMS: a double-blind, sham-controlled study. Eur. Arch. Psychiatry Clin. Neurosci. 263, 475–484. https://doi.org/10.1007/s00406-012-0368-x

Knecht, S., Sommer, J., Deppe, M., Steinsträter, O., 2005. Scalp position and efficacy of transcranial magnetic stimulation. Clin. Neurophysiol. 116, 1988–1993. https://doi.org/10.1016/j.clinph.2005.04.016

Kochenderfer, M.J., Wheeler, T.A., 2019. Algorithms for Optimization. The MIT Press, Cambridge.

Komssi, S., Kähkönen, S., Ilmoniemi, R.J., 2004. The effect of stimulus intensity on brain responses evoked by transcranial magnetic stimulation. Hum. Brain Mapp. 21, 154–164. https://doi.org/10.1002/hbm.10159

Koponen, L.M., Nieminen, J.O., Ilmoniemi, R.J., 2018. Multi-locus transcranial magnetic stimulation—theory and implementation. Brain Stimul. 11, 849–855. https://doi.org/10.1016/j.brs.2018.03.014

Krieg, S.M., Lioumis, P., Mäkelä, J.P., Wilenius, J., Karhu, J., Hannula, H., Savolainen, P., Lucas, C.W., Seidel, K., Laakso, A., Islam, M., Vaalto, S., Lehtinen, H., Vitikainen, A.M., Tarapore, P.E., Picht, T., 2017. Protocol for motor and language mapping by navigated TMS in patients and healthy volunteers; workshop report. Acta Neurochir. 159, 1187–1195. https://doi.org/10.1007/s00701-017-3187-z

Krige, D.G., 1951. A statistical approach to some basic mine valuation problems on the Withwaterstrand. J. Chem. Metall. Min. Soc. South Africa 52, 119–139.

Kujirai, T., Caramia, M.D., Rothwell, J.C., Day, B.L., Thompson, P.D., Ferbert, A., Wroe, S., Asselman, P., Marsden, C.D., 1993. Corticocortical inhibition in human motor cortex. J. Physiol. 471, 501–519. https://doi.org/10.1113/jphysiol.1993.sp019912

Laakso, I., Hirata, A., Ugawa, Y., 2014. Effects of coil orientation on the electric field induced by TMS over the hand motor area. Phys. Med. Biol. 59, 203–218. https://doi.org/10.1088/0031-9155/59/1/203

Laine, M., 2021. Corticocortical modulation of motor responses with multi-locus transcranial magnetic stimulation. Master's Thesis. Aalto University, Espoo, Finland. https://aaltodoc.aalto.fi/handle/123456789/112456.

Lancaster, J.L., Narayana, S., Wenzel, D., Luckemeyer, J., Roby, J., Fox, P., 2004. Evaluation of an image-guided, robotically positioned transcranial magnetic stimulation system. Hum. Brain Mapp. 22, 329–340. https://doi.org/10.1002/hbm.20041

Lebossé, C., Renaud, P., Bayle, B., De Mathelin, M., Piccin, O., Foucher, J., 2007. A robotic system for automated image-guided transcranial magnetic stimulation. IEEE/NIH Life Sci. Syst. Appl. Work. 55–58. https://doi.org/10.1109/LSSA.2007.4400883

Lefaucheur, J.-P., Aleman, A., Baeken, C., Benninger, D.H., Brunelin, J., Di Lazzaro, V., Filipović, S.R., Grefkes, C., Hasan, A., Hummel, F.C., Jääskeläinen, S.K., Langguth, B., Leocani, L., Londero, A., Nardone, R., Nguyen, J.-P., Nyffeler, T., Oliveira-Maia, A.J., Oliviero, A., Padberg, F., Palm, U., Paulus, W., Poulet, E., Quartarone, A., Rachid, F., Rektorová, I., Rossi, S., Sahlsten, H., Schecklmann, M., Szekely, D., Ziemann, U., 2020. Evidence-based guidelines on the therapeutic use of repetitive transcranial magnetic stimulation (rTMS): an update (2014–2018). Clin. Neurophysiol. 131, 474–528. https://doi.org/10.1016/j.clinph.2019.11.002

Lefaucheur, J.-P., Picht, T., 2016. The value of preoperative functional cortical mapping using navigated TMS. Neurophysiol. Clin. 46, 125–133. https://doi.org/10.1016/j.neucli.2016.05.001

Lioumis, P., Zhdanov, A., Mäkelä, N., Lehtinen, H., Wilenius, J., Neuvonen, T., Hannula, H., Deletis, V., Picht, T., Mäkelä, J.P., 2012. A novel approach for documenting naming errors induced by navigated transcranial magnetic stimulation. J. Neurosci. Methods 204, 349–354. https://doi.org/10.1016/j.jneumeth.2011.11.003

Maccabee, P.J., Amassian, V.E., Eberle, L.P., Cracco, R.Q., 1993. Magnetic coil stimulation of straight and bent amphibian and mammalian peripheral nerve in vitro: locus of excitation. J. Physiol. 460, 201–219. https://doi.org/10.1113/jphysiol.1993.sp019467

Magistris, M.R., Rösler, K.M., Truffert, A., Myers, J.P., 1998. Transcranial stimulation excites virtually all motor neurons supplying the target muscle: a demonstration and a method improving the study of motor evoked potentials. Brain 121, 437–450. https://doi.org/10.1093/brain/121.3.437

Mascott, C.R., Sol, J.-C., Bousquet, P., Lagarrigue, J., Lazorthes, Y., Lauwers-Cances, V., 2006. Quantification of true in vivo (application) accuracy in cranial image-guided surgery: influence of mode of patient registration. Oper. Neurosurg. 59, 146–147. https://doi.org/10.1227/01.NEU.0000220089.39533.4E

Maurer Jr, C.R., Rohlfing, T., Dean, D., West, J.B., Rueckert, D., Mori, K., Shahidi, R., Martin, D.P., Heilbrun, M.P., Maciunas, R.J., 2002. Sources of error in image registration for cranial image-guided neurosurgery, in: Germano, I.M. (Ed.), Advanced Techniques in Image-Guided Brain and Spine Surgery. Thieme, New York, pp. 10–36.

Meincke, J., Hewitt, M., Batsikadze, G., Liebetanz, D., 2016. Automated TMS hotspot-hunting using a closed loop threshold-based algorithm. Neuroimage 124, 509–517. https://doi.org/10.1016/j.neuroimage.2015.09.013

Meyer, B.U., Diehl, R., Steinmetz, H., Britton, T.C., Benecke, R., 1991. Magnetic stimuli applied over motor and visual cortex: influence of coil position and field polarity on motor responses, phosphenes, and eye movements. Electroencephalogr. Clin. Neurophysiol. Suppl. 43, 121–134.

Mikkonen, M., Laakso, I., 2019. Effects of posture on electric fields of non-invasive brain stimulation. Phys. Med. Biol. 64, 065019. https://doi.org/10.1088/1361-6560/ab03f5

Mills, K.R., Boniface, S.J., Schubert, M., 1992. Magnetic brain stimulation with a double coil: the importance of coil orientation. Electroencephalogr. Clin. Neurophysiol. 85, 17–21. https://doi.org/10.1016/0168-5597(92)90096-T

Miranda, P.C., De Carvalho, M., Conceição, I., Sales Luis, M.L., Ducla-Soares, E., 1997. A new method for reproducible coil positioning in transcranial magnetic stimulation mapping. Electroencephalogr. Clin. Neurophysiol. 105, 116–123. https://doi.org/10.1016/S0924-980X(97)95720-9

Mutanen, T., Mäki, H., Ilmoniemi, R.J., 2013. The effect of stimulus parameters on TMS–EEG muscle artifacts. Brain Stimul. 6, 371–376. https://doi.org/10.1016/j.brs.2012.07.005

Mutanen, T.P., Biabani, M., Sarvas, J., Ilmoniemi, R.J., Rogasch, N.C., 2020. Source-based artifact-rejection techniques available in TESA, an open-source TMS–EEG toolbox. Brain Stimul. 13, 1349–1351. https://doi.org/10.1016/j.brs.2020.06.079

Mutanen, T.P., Metsomaa, J., Liljander, S., Ilmoniemi, R.J., 2018. Automatic and robust noise suppression in EEG and MEG: the SOUND algorithm. Neuroimage 166, 135–151. https://doi.org/10.1016/j.neuroimage.2017.10.021

Mutanen, T.P., Souza, V.H., Nieminen, J.O., Ilmoniemi, R.J., 2021. On the effective resolution of TMS, its tradeoff with signal-to-noise ratio, and the experimental implications. Int. J. Bioelectromagn. 23, 13/1–4.

Navarro de Lara, L.I., Daneshzand, M., Mascarenas, A., Paulson, D., Pratt, K., Okada, Y., Raij, T., Makarov, S.N., Nummenmaa, A., 2021. A 3-axis coil design for multichannel TMS arrays. Neuroimage 224, 117355. https://doi.org/10.1016/j.neuroimage.2020.117355

Neggers, S.F.W., Langerak, T.R., Schutter, D.J.L.G., Mandl, R.C.W., Ramsey, N.F., Lemmens, P.J.J., Postma, A., 2004. A stereotactic method for image-guided transcranial magnetic stimulation validated with fMRI and motor-evoked potentials. Neuroimage 21, 1805–1817. https://doi.org/10.1016/j.neuroimage.2003.12.006

Niehaus, L., Meyer, B.-U., Weyh, T., 2000. Influence of pulse configuration and direction of coil current on excitatory effects of magnetic motor cortex and nerve stimulation. Clin. Neurophysiol. 111, 75–80. https://doi.org/10.1016/S1388-2457(99)00198-4

Nielsen, J.D., Madsen, K.H., Puonti, O., Siebner, H.R., Bauer, C., Madsen, C.G., Saturnino, G.B., Thielscher, A., 2018. Automatic skull segmentation from MR images for realistic volume conductor models of the head: assessment of the state-of-the-art. Neuroimage 174, 587–598. https://doi.org/10.1016/j.neuroimage.2018.03.001

Nieminen, J.O., Koponen, L.M., Mäkelä, N., Souza, V.H., Stenroos, M., Ilmoniemi, R.J., 2019. Short-interval intracortical inhibition in human primary motor cortex: a multi-locus transcranial magnetic stimulation study. Neuroimage 203, 116194. https://doi.org/10.1016/j.neuroimage.2019.116194

Noccaro, A., Mioli, A., D'Alonzo, M., Pinardi, M., Di Pino, G., Formica, D., 2021. Development and validation of a novel calibration methodology and control approach for robot-aided transcranial magnetic stimulation (TMS). IEEE Trans. Biomed. Eng. 68, 1589–1600. https://doi.org/10.1109/TBME.2021.3055434

Nummenmaa, A., Stenroos, M., Ilmoniemi, R.J., Okada, Y.C., Hämäläinen, M.S., Raij, T., 2013. Comparison of spherical and realistically shaped boundary element head models for transcranial magnetic stimulation navigation. Clin. Neurophysiol. 124, 1995–2007. https://doi.org/10.1016/j.clinph.2013.04.019

Nurmi, S., Karttunen, J., Souza, V.H., Ilmoniemi, R.J., Nieminen, J.O., 2021. Trade-off between stimulation focality and the number of coils in multi-locus transcranial magnetic stimulation. J. Neural Eng. 18, 066003. https://doi.org/10.1088/1741-2552/ac3207

Olesen, O.V., Jørgensen, M.R., Paulsen, R.R., Højgaard, L., Roed, B., Larsen, R., 2010. Structured light 3D tracking system for measuring motions in PET brain imaging. Proc. SPIE, Med. Imaging 2010 Vis. Image-Guided Proced. Model. 76250X. https://doi.org/10.1117/12.845060

Opitz, A., Legon, W., Rowlands, A., Bickel, W.K., Paulus, W., Tyler, W.J., 2013. Physiological observations validate finite element models for estimating subject-specific electric field distributions induced by transcranial magnetic stimulation of the human motor cortex. Neuroimage 81, 253–264. https://doi.org/10.1016/j.neuroimage.2013.04.067

Pascual-Leone, A., Gates, J.R., Dhuna, A., 1991. Induction of speech arrest and counting errors with rapid-rate transcranial magnetic stimulation. Neurology 41, 697–702. https://doi.org/10.1212/WNL.41.5.697

Pascual-Leone, A., Rubio, B., Pallardó, F., Catalá, M.D., 1996. Rapid-rate transcranial magnetic stimulation of left dorsolateral prefrontal cortex in drug-resistant depression. Lancet 348, 233–237. https://doi.org/10.1016/S0140-6736(96)01219-6

Pascual-Leone, A., Walsh, V., Rothwell, J., 2000. Transcranial magnetic stimulation in cognitive neuroscience – virtual lesion, chronometry, and functional connectivity. Curr. Opin. Neurobiol. 10, 232–237. https://doi.org/10.1016/S0959-4388(00)00081-7

Peterchev, A.V., D'Ostilio, K., Rothwell, J.C., Murphy, D.L., 2014. Controllable pulse parameter transcranial magnetic stimulator with enhanced circuit topology and pulse shaping. J. Neural Eng. 11, 056023. https://doi.org/10.1088/1741-2560/11/5/056023

Picheny, V., Wagner, T., Ginsbourger, D., 2013. A benchmark of kriging-based infill criteria for noisy optimization. Struct. Multidiscip. Optim. 48, 607–626. https://doi.org/10.1007/s00158-013-0919-4

Picht, T., Krieg, S.M., Sollmann, N., Rösler, J., Niraula, B., Neuvonen, T., Savolainen, P., Lioumis, P., Mäkelä, J.P., Deletis, V., Meyer, B., Vajkoczy, P., Ringel, F., 2013. A comparison of language mapping by preoperative navigated transcranial magnetic stimulation and direct cortical stimulation during awake surgery. Neurosurgery 72, 808–819. https://doi.org/10.1227/NEU.0b013e3182889e01

Picht, T., Schmidt, S., Brandt, S., Frey, D., Hannula, H., Neuvonen, T., Karhu, J., Vajkoczy, P., Suess, O., 2011. Preoperative functional mapping for rolandic brain tumor surgery: comparison of navigated transcranial magnetic stimulation to direct cortical stimulation. Neurosurgery 69, 581–589. https://doi.org/10.1227/NEU.0b013e3182181b89

Pitcher, J.B., Ogston, K.M., Miles, T.S., 2003. Age and sex differences in human motor cortex input–output characteristics. J. Physiol. 546, 605–613. https://doi.org/10.1113/jphysiol.2002.029454

Plewnia, C., Reimold, M., Najib, A., Brehm, B., Reischl, G., Plontke, S.K., Gerloff, C., 2007. Dose-dependent attenuation of auditory phantom perception (tinnitus) by PET-guided repetitive transcranial magnetic stimulation. Hum. Brain Mapp. 28, 238–246. https://doi.org/10.1002/hbm.20270

Raffin, E., Harquel, S., Passera, B., Chauvin, A., Bougerol, T., David, O., 2020. Probing regional cortical excitability via input–output properties using transcranial magnetic stimulation and electroencephalography coupling. Hum. Brain Mapp. 41, 2741–2761. https://doi.org/10.1002/hbm.24975

Rashed, E.A., Gomez-Tames, J., Hirata, A., 2021. Influence of segmentation accuracy in structural MR head scans on electric field computation for TMS and tES. Phys. Med. Biol. 66, 064002. https://doi.org/10.1088/1361-6560/abe223

Rasmussen, C.E., Williams, C.K.I., 2006. Gaussian Processes for Machine Learning. The MIT Press, Cambridge.

Richter, L., 2013. Robotized Transcranial Magnetic Stimulation, Springer. New York. https://doi.org/10.1007/978-1-4614-7360-2

Richter, L., Matthäus, L., Schlaefer, A., Schweikard, A., 2010. Fast robotic compensation of spontaneous head motion during transcranial magnetic stimulation (TMS). UKACC Int. Conf. Control 872 – 877. https://doi.org/10.1049/ic.2010.0396

Richter, L., Trillenberg, P., Schweikard, A., Schlaefer, A., 2013. Stimulus intensity for hand held and robotic transcranial magnetic stimulation. Brain Stimul. 6, 315–321. https://doi.org/10.1016/j.brs.2012.06.002

Ridding, M.C., Ziemann, U., 2010. Determinants of the induction of cortical plasticity by non-invasive brain stimulation in healthy subjects. J. Physiol. 588, 2291–2304. https://doi.org/10.1113/jphysiol.2010.190314

Rogasch, N.C., Sullivan, C., Thomson, R.H., Rose, N.S., Bailey, N.W., Fitzgerald, P.B., Farzan, F., Hernandez-Pavon, J.C., 2017. Analysing concurrent transcranial magnetic stimulation and electroencephalographic data: a review and introduction to the open-source TESA software. Neuroimage 147, 934–951. https://doi.org/10.1016/j.neuroimage.2016.10.031

Rosanova, M., Casali, A., Bellina, V., Resta, F., Mariotti, M., Massimini, M., 2009. Natural frequencies of human corticothalamic circuits. J. Neurosci. 29, 7679–7685. https://doi.org/10.1523/JNEUROSCI.0445-09.2009

Rosin, B., Slovik, M., Mitelman, R., Rivlin-Etzion, M., Haber, S.N., Israel, Z., Vaadia, E., Bergman, H., 2011. Closed-loop deep brain stimulation is superior in ameliorating Parkinsonism. Neuron 72, 370–384. https://doi.org/10.1016/j.neuron.2011.08.023

Rossini, P.M., Burke, D., Chen, R., Cohen, L.G., Daskalakis, Z., Di Iorio, R., Di Lazzaro, V., Ferreri, F., Fitzgerald, P.B., George, M.S., Hallett, M., Lefaucheur, J.P., Langguth, B., Matsumoto, H., Miniussi, C., Nitsche, M.A., Pascual-Leone, A., Paulus, W., Rossi, S., Rothwell, J.C., Siebner, H.R., Ugawa, Y., Walsh, V., Ziemann, U., 2015. Non-invasive electrical and magnetic stimulation of the brain, spinal cord, roots and peripheral nerves: basic principles and procedures for routine clinical and research application: An updated report from an I.F.C.N. Committee. Clin. Neurophysiol. 126, 1071–1107. https://doi.org/10.1016/j.clinph.2015.02.001

Rotenberg, A., 2010. Prospects for clinical applications of transcranial magnetic stimulation and real-time EEG in epilepsy. Brain Topogr. 22, 257–266. https://doi.org/10.1007/s10548-009-0116-3

Ruohonen, J., Ilmoniemi, R.J., 1998. Focusing and targeting of magnetic brain stimulation using multiple coils. Med. Biol. Eng. Comput. 36, 297–301. https://doi.org/10.1007/BF02522474

Ruohonen, J., Karhu, J., 2010. Navigated transcranial magnetic stimulation. Neurophysiol. Clin. 40, 7–17. https://doi.org/10.1016/j.neucli.2010.01.006

Saari, J., Kallioniemi, E., Tarvainen, M., Julkunen, P., 2018. Oscillatory TMS-EEG-responses as a measure of the cortical excitability threshold. IEEE Trans. Neural Syst. Rehabil. Eng. 26, 383–391. https://doi.org/10.1109/TNSRE.2017.2779135

Salinas, F.S., Lancaster, J.L., Fox, P.T., 2009. 3D modeling of the total electric field induced by transcranial magnetic stimulation using the boundary element method. Phys. Med. Biol. 54, 3631–3647. https://doi.org/10.1088/0031-9155/54/12/002

Sano, S., Kadowaki, T., Tsuda, K., Kimura, S., 2020. Application of Bayesian optimization for pharmaceutical product development. J. Pharm. Innov. 15, 333–343. https://doi.org/10.1007/s12247-019-09382-8

Saturnino, G.B., Thielscher, A., Madsen, K.H., Knösche, T.R., Weise, K., 2019. A principled approach to conductivity uncertainty analysis in electric field calculations. Neuroimage 188, 821–834. https://doi.org/10.1016/j.neuroimage.2018.12.053

Schönfeldt-Lecuona, C., Thielscher, A., Freudenmann, R.W., Kron, M., Spitzer, M., Herwig, U., 2005. Accuracy of stereotaxic positioning of transcranial magnetic stimulation. Brain Topogr. 17, 253–259. https://doi.org/10.1007/s10548-005-6033-1

Shahriari, B., Swersky, K., Wang, Z., Adams, R.P., de Freitas, N., 2016. Taking the human out of the loop: a review of Bayesian optimization. Proc. IEEE 104, 148–175. https://doi.org/10.1109/JPROC.2015.2494218

Siebner, H.R., Peller, M., Lee, L., 2003. Applications of combined TMS–PET studies in clinical and basic research. Suppl. Clin. Neurophysiol. 56, 63–72. https://doi.org/10.1016/S1567-424X(09)70210-7

Sollmann, N., Goblirsch-Kolb, M.F., Ille, S., Butenschoen, V.M., Boeckh-Behrens, T., Meyer, B., Ringel, F., Krieg, S.M., 2016. Comparison between electric-field-navigated and line-navigated TMS for cortical motor mapping in patients with brain tumors. Acta Neurochir. 158, 2277–2289. https://doi.org/10.1007/s00701-016-2970-6

Sondergaard, R.E., Martino, D., Kiss, Z.H.T., Condliffe, E.G., 2021. TMS motor mapping methodology and reliability: a structured review. Front. Neurosci. 15, 709368. https://doi.org/10.3389/fnins.2021.709368

Souza, V.H., Nieminen, J.O., Tugin, S., Koponen, L.M., Baffa, O., Ilmoniemi, R.J., 2022. TMS with fast and accurate electronic control: measuring the orientation sensitivity of corticomotor pathways. Brain Stimul. 15, 306–315. https://doi.org/10.1016/j.brs.2022.01.009

Sparing, R., Buelte, D., Meister, I.G., Pauš, T., Fink, G.R., 2008. Transcranial magnetic stimulation and the challenge of coil placement: a comparison of conventional and stereotaxic neuronavigational strategies. Hum. Brain Mapp. 29, 82–96. https://doi.org/10.1002/hbm.20360

Stenroos, M., Koponen, L.M., 2019. Real-time computation of the TMS-induced electric field in a realistic head model. Neuroimage 203, 116159. https://doi.org/10.1016/j.neuroimage.2019.116159

Stewart, L.M., Walsh, V., Rothwell, J.C., 2001. Motor and phosphene thresholds: a transcranial magnetic stimulation correlation study. Neuropsychologia 39, 415–419. https://doi.org/10.1016/S0028-3932(00)00130-5

Stokes, M.G., Chambers, C.D., Gould, I.C., English, T., McNaught, E., McDonald, O., Mattingley, J.B., 2007. Distance-adjusted motor threshold for transcranial magnetic stimulation. Clin. Neurophysiol. 118, 1617–1625. https://doi.org/10.1016/j.clinph.2007.04.004

Thielscher, A., Opitz, A., Windhoff, M., 2011. Impact of the gyral geometry on the electric field induced by transcranial magnetic stimulation. Neuroimage 54, 234–243. https://doi.org/10.1016/j.neuroimage.2010.07.061

Torfeh, T., Hammoud, R., Perkins, G., McGarry, M., Aouadi, S., Celik, A., Hwang, K.-P., Stancanello, J., Petric, P., Al-Hammadi, N., 2016. Characterization of 3D geometric distortion of magnetic resonance imaging scanners commissioned for radiation therapy planning. Magn. Reson. Imaging 34, 645–653. https://doi.org/10.1016/j.mri.2016.01.001

Trapp, N.T., Bruss, J., King Johnson, M., Uitermarkt, B.D., Garrett, L., Heinzerling, A., Wu, C., Koscik, T.R., Ten Eyck, P., Boes, A.D., 2020. Reliability of targeting methods in TMS for depression: Beam F3 vs. 5.5 cm. Brain Stimul. 13, 578–581. https://doi.org/10.1016/j.brs.2020.01.010

Tremblay, S., Rogasch, N.C., Premoli, I., Blumberger, D.M., Casarotto, S., Chen, R., Di Lazzaro, V., Farzan, F., Ferrarelli, F., Fitzgerald, P.B., Hui, J., Ilmoniemi, R.J., Kimiskidis, V.K., Kugiumtzis, D., Lioumis, P., Pascual-Leone, A., Pellicciari, M.C., Rajji, T., Thut, G., Zomorrodi, R., Ziemann, U., Daskalakis, Z.J., 2019. Clinical utility and prospective of TMS–EEG. Clin. Neurophysiol. 130, 802–844. https://doi.org/10.1016/j.clinph.2019.01.001

Triggs, W.J., Calvanio, R., Macdonell, R.A.L., Cros, D., Chiappa, K.H., 1994. Physiological motor asymmetry in human handedness: evidence from transcranial magnetic stimulation. Brain Res. 636, 270–276. https://doi.org/10.1016/0006-8993(94)91026-x

Triggs, W.J., Subramanium, B., Rossi, F., 1999. Hand preference and transcranial magnetic stimulation asymmetry of cortical motor representation. Brain Res. 835, 324–329. https://doi.org/10.1016/S0006-8993(99)01629-7

Ueno, S., Tashiro, T., Harada, K., 1988. Localized stimulation of neural tissues in the brain by means of a paired configuration of time-varying magnetic fields. J. Appl. Phys. 64, 5862–5864. https://doi.org/10.1063/1.342181

van Bueren, N.E.R., Reed, T.L., Nguyen, V., Sheffield, J.G., van der Ven, S.H.G., Osborne, M.A., Kroesbergen, E.H., Kadosh, R.C., 2021. Personalized brain stimulation for effective neurointervention across participants. PLoS Comput. Biol. 17, e1008886. https://doi.org/10.1371/journal.pcbi.1008886

Vernet, M., Thut, G., 2014. Electroencephalography during transcranial magnetic stimulation: current modus operandi, in: Pascual-Leone, A., Horvath, J.C., Rotenberg, A. (Eds.), Transcranial Magnetic Stimulation. Humana Press, New York, pp. 197–232. https://doi.org/10.1007/978-1-4939-0879-0_11

Virtanen, J., Ruohonen, J., Näätänen, R., Ilmoniemi, R.J., 1999. Instrumentation for the measurement of electric brain responses to transcranial magnetic stimulation. Med. Biol. Eng. Comput. 37, 322–326. https://doi.org/10.1007/BF02513307

Walsh, V., Cowey, A., 2000. Transcranial magnetic stimulation and cognitive neuroscience. Nat. Rev. Neurosci. 1, 73–80. https://doi.org/10.1038/35036239

Wang, M.N., Song, Z.J., 2011. Classification and analysis of the errors in neuronavigation. Neurosurgery 68, 1131–1143. https://doi.org/10.1227/NEU.0b013e318209cc45

Weise, K., Numssen, O., Thielscher, A., Hartwigsen, G., Knösche, T.R., 2020. A novel approach to localize cortical TMS effects. Neuroimage 209, 116486. https://doi.org/10.1016/j.neuroimage.2019.116486

West, J.B., Maurer Jr., C.R., 2004. Designing optically tracked instruments for image-guided surgery. IEEE Trans. Med. Imaging 23, 533–545. https://doi.org/10.1109/TMI.2004.825614

Wiles, A.D., Thompson, D.G., Frantz, D.D., 2004. Accuracy assessment and interpretation for optical tracking systems. Proc. SPIE, Med. Imaging 2004 Vis. Image-Guided Proced. Disp. 5367, 421–432. https://doi.org/10.1117/12.536128

Windhoff, M., Opitz, A., Thielscher, A., 2013. Electric field calculations in brain stimulation based on finite elements: an optimized processing pipeline for the generation and usage of accurate individual head models. Hum. Brain Mapp. 34, 923–935. https://doi.org/10.1002/hbm.21479

Yi, X., Bicker, R., 2010. Design of a robotic transcranial magnetic stimulation system. 2010 IEEE Conf. Robot. Autom. Mechatronics 78–83. https://doi.org/10.1109/RAMECH.2010.5513208

Zaidi, T.A., Makarov, S.N., Fujimoto, K., 2021. Electric field comparison for TMS using different neuroimaging segmentation methods. Proc. Annu. Int. Conf. IEEE Eng. Med. Biol. Soc. 6565–6568. https://doi.org/10.1109/EMBC46164.2021.9630719

Zhang, H., Gomez, L.J., Guilleminot, J., 2022. Uncertainty quantification of TMS simulations considering MRI segmentation errors. J. Neural Eng. 19, 026022. https://doi.org/10.1088/1741-2552/ac52d1

Ziemann, U., Reis, J., Schwenkreis, P., Rosanova, M., Strafella, A., Badawy, R., Müller-Dahlhaus, F., 2015. TMS and drugs revisited 2014. Clin. Neurophysiol. 126, 1847–1868. https://doi.org/10.1016/j.clinph.2014.08.028

Ziemann, U., Rothwell, J.C., Ridding, M.C., 1996. Interaction between intracortical inhibition and facilitation in human motor cortex. J. Physiol. 496, 873–881. https://doi.org/10.1113/jphysiol.1996.sp021734

Zrenner, C., Belardinelli, P., Müller-Dahlhaus, F., Ziemann, U., 2016. Closed-loop neuroscience and non-invasive brain stimulation: a tale of two loops 10, 92. https://doi.org/10.3389/fncel.2016.00092

Zrenner, C., Desideri, D., Belardinelli, P., Ziemann, U., 2018. Real-time EEG-defined excitability states determine efficacy of TMS-induced plasticity in human motor cortex. Brain Stimul. 11, 374–389. https://doi.org/10.1016/j.brs.2017.11.016

Aalto-DT 77/2022

ISBN 978-952-64-0820-0 (printed)
ISBN 978-952-64-0821-7 (pdf)
ISSN 1799-4934 (printed)
ISSN 1799-4942 (pdf)

Aalto University
School of Science
Department of Neuroscience and Biomedical Engineering
www.aalto.fi

BUSINESS + ECONOMY

ART + DESIGN + ARCHITECTURE

SCIENCE + TECHNOLOGY

CROSSOVER

DOCTORAL THESES